Relationship between the Structure and the DNA Binding Properties of Diazoniapolycyclic Duplex- and Triplex-DNA Binders: Efficiency, Selectivity, and Binding Mode†

Serena Basili,‡ Anna Bergen,§ Francesco Dall'Acqua,‡ Anita Faccio,‡ Anton Granzhan,§ Heiko Ihmels,*,§ Stefano Moro,‡ and Giampietro Viola‡

Organic Chemistry II, University of Siegen, Adolf-Reichwein-Strasse 2, D-57068 Siegen, Germany, and Department of Pharmaceutical Sciences, University of Padova, via Marzolo 5, I-35131 Padova, Italy

Received July 30, 2007; Revised Manuscript Received August 23, 2007

ABSTRACT: The association of dicationic polycyclic ligands, namely, four diazoniapentaphene derivatives, three diazoniaanthra[1,2-*a*]anthracenes, diazoniahexaphene, and a partly saturated hydroxy-substituted diazoniapentaphene with double-stranded and triple-helical DNA, was investigated by spectrophotometric and viscosimetric titrations, CD and LD spectroscopy, DNA melting experiments, and molecular modeling studies. All experimental and theoretical data reveal an intercalative DNA-binding mode of the diazoniapentaphenes and diazoniaanthra[1,2-*a*]anthracenes; the latter have approximately 10-fold higher affinity for the DNA duplex. CD spectroscopic investigations and molecular modeling studies show that only one azonianaphthalene part of the ligand is intercalated between the DNA base pairs, whereas the remaining part of the ligand points outside the intercalation pocket. In contrast, the diazoniahexaphene is a DNA groove binder, which binds selectively to $[poly(dAdT)]_2$. At low ligand-to-DNA ratios ($r < 0.15$), the diazoniahexaphene also behaves as an intercalator; however, all spectroscopic and viscosimetric data are consistent with significant groove binding of this ligand at $r > 0.2$. Studies of the interaction of diazoniapolycyclic ions with triplex DNA reveal a preferential binding of both diazoniapentaphenes and diazoniaanthra[1,2-*a*]anthracenes to the triplex and stabilization thereof. These properties are more pronounced in the case of the hexacyclic diazoniaanthra[1,2-*a*]anthracenes; however, the diazoniahexaphene shows no preferential binding to the triplex. The DNA binding properties of the diazoniapentaphene derivatives remain essentially the same upon variation of the positions of nitrogen atoms or substitution with methyl groups. In contrast, the interactions of the diazoniaanthra[1,2-*a*]anthracence isomers with triplex DNA are slightly different. Notably, the 14a,16a-diazoniaanthra[1,2-*a*]anthracene is among the most efficient triplex stabilizers, with a 9-fold larger binding affinity for the triplex than for the DNA duplex. Moreover, the diazoniapentaphene and diazoniaanthra[1,2-*a*]anthracene derivatives represent the first examples of triplex-DNA binders that do not require additional aminoalkyl side chains for efficient triplex stabilization.

The investigation of the interactions of nucleic acids with small-molecule ligands is an active research area, and the latter compounds represent targets for drug design in anticancer therapy (*1*, *2*). Along these lines, especially important are the ligands capable of structure- or sequence-selective binding to nucleic acids, since such compounds may purposefully influence the biological functionality of genetic material in vivo (*3*).

The condensed poly(hetero)aromatic compounds are usually regarded as representative DNA intercalators, especially if they possess electron-deficient or charged aromatic cores (*4*). However, only a few ligands are known that bind to the DNA by the intercalative mode exclusively, i.e., by insertion between the neighboring base pairs of DNA. A vast number of ligands, which have an intercalating part endowed with a variety of substituents, bind to the DNA by a mixed mode, since the substituents occupy the DNA grooves upon binding and thus determine the selectivity and binding energetics of the ligand. Thus, in the case of the "classical" intercalator ethidium, the phenyl ring occupies the minor groove, resulting in an overall heterogeneous DNA binding (*5*, *6*). At the same time, even relatively small changes in the structure of the ligands may lead to the inversion of the binding mode or complete suppression of DNA binding, which has been shown for the ethidium derivatives (*7*, *8*) and substituted 9-methylacridinium salts (*9*). The effect of the side chains containing amino and hydroxy substituents on the DNA affinity and binding mode of mono- and disubstituted anthracenes has been systematically investigated (*10*−*12*).

† H.I. and A.G. thank the Deutsche Forschungsgemeinschaft for generous financial support. S.M. thanks the University of Padova, Italy, and the Italian Ministry for University and Research (MIUR), Rome, Italy, for financial support, and the Chemical Computing Group for the scientific and technical partnership.

* To whom correspondence should be addressed. E-mail: ihmels@chemie.uni-siegen.de. Fax: +49 (0) 271 740 4052. Phone: +49 (0) 271 740 3440.

‡ University of Padova.

§ University of Siegen.

10.1021/bi701518v CCC: $37.00
Published on Web 10/16/2007

Chart 1: Structures of Annelated Quinolizinium Ions **1**−**3** and Diazoniapolycyclic Ions **4**−**7**

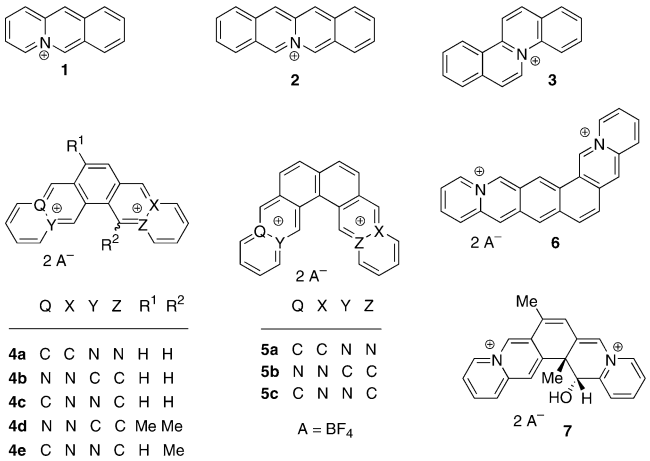

	Q	X	Y	Z	R^1	R^2
4a	C	C	N	N	H	H
4b	N	N	C	C	H	H
4c	C	N	N	C	H	H
4d	N	N	C	C	Me	Me
4e	C	N	N	C	H	Me

	Q	X	Y	Z
5a	C	C	N	N
5b	N	N	C	C
5c	C	N	N	C

In view of the complexity of the ligand−DNA recognition process, a study with model compounds, which possess only one DNA-binding mode, is desired. Such an investigation might reveal the base or sequence preference of the intercalating chromophore, unmodified by the side-chain substituents. However, the investigation of the DNA binding properties of unsubstituted arenes and heteroarenes, such as anthracene, pyrene, and acridine, is hampered by their low solubility in water, and the attachment of the water-soluble side groups, which at the same time may influence the DNA binding properties, is necessary (*13*−*15*). We have shown earlier that the quinolizinium cation represents a promising platform for the DNA-binding ligands, since the annelated derivatives of this ion are very water-soluble due to the presence of an intrinsic positive charge (*16*). Thus, benzo[*b*]quinolizinium (acridizinium) cation (**1**) (Chart 1) and naphthoquinolizinium derivatives are unsubstituted heteroaromatic compounds, capable of binding to double-stranded DNA (dsDNA) (*17, 18*). A combination of spectrophotometric and spectrofluorimetric titrations, linear and circular dichroism spectroscopy, and primer-extension analysis was used to show that these compounds bind to the DNA by a combination of intercalation and association with the phosphate backbone, with a slight preference for GC-rich over AT-rich DNA regions (*18*). Recently, we have extended our studies of unsubstituted cationic heterocycles to other four-ring polyacenes, namely, linear and angular dibenzoquinolizinium derivatives **2** and **3**, which may be considered as water-soluble analogues of tetracene and chrysene, respectively (*19*). We have demonstrated that both derivatives exhibit an intercalative mode of binding to dsDNA with moderate binding constants ($K = 1-7 \times 10^5$ M^{-1}) and a slight preference for association with GC-rich DNA regions. At the same time, both derivatives preferentially bind to the triple-helical DNA over the duplex form, although the affinity and selectivity of the binding depend significantly on the shape of the aromatic system.

In the context of our investigations of polyannelated quinolizinium derivatives, we have prepared and investigated a range of polyheterocycles (diazoniapolycyclic ions) containing two quinolizinium fragments and consequently a dicationic chromophore (*20*−*25*). Our preliminary studies have shown that the compounds of this type, such as 12a, 14a-diazoniapentaphene **4a**, have an increased affinity for dsDNA, as compared with the monocharged derivatives, in combination with an almost exclusive intercalative binding mode (*26*). Moreover, a significant preferential binding to the triple-helical DNA poly(dA)-$[poly(dT)]_2$ was observed, most pronounced in the case of diazoniaanthra[1,2-*a*]anthracenes **5a** and **5b** (*27*). Herein, we report a systematic investigation of the DNA binding properties of an extended series of diazoniapolycyclic salts (termed "DAPS"), including the unsubstituted and methyl-substituted diazoniapentaphenes **4a**−**e**, the three isomeric diazoniaanthra[1,2-*a*]anthracenes **5a**−**c**, the recently described diazoniahexaphene **6**, and a partly saturated, hydroxy-substituted diazoniapentaphene derivative **7**. With this series in hand, we tried to establish the influence of (i) the shape of the ligand (angular, **4a**−**e** and **6**, and helicene-like, **5a**−**c**), (ii) the position of the bridgehead nitrogen atoms, and (iii) the methyl substituents on the DNA binding properties of DAPS with respect to duplex and triple-helical DNA, and we used a combination of the physicochemical techniques, such as spectrophotometric titrations, linear (LD) and circular dichroism (CD) spectroscopy, viscosimetric experiments, DNA thermal denaturation studies, and molecular modeling, to achieve this goal.

EXPERIMENTAL PROCEDURES

Ligands and Buffer Solutions. Synthesis and characterization of the investigated compounds have been described previously (*20*−*25*). The identity and purity of all ligands were confirmed by ^1H and ^{13}C NMR spectroscopy and elemental analysis data. Stock solutions of all ligands (1 mM) were prepared in HPLC-grade DMSO or acetonitrile. All buffer solutions were prepared from purified water (resistivity of 18 MΩ cm^{-1}) and biochemistry-grade chemicals. Prior to use, the buffer solutions were filtered through a PVDF membrane filter (pore size of 0.45 μm). ETN buffer [10 mM TRIS, 1 mM EDTA, and 10 mM NaCl (pH 7.0)] or BPE buffer [6.0 mM Na_2HPO_4, 2.0 mM NaH_2PO_4, and 1.0 mM Na_2EDTA, with a total Na^+ concentration of 16.0 mM (pH 7.0)] was used for thermal denaturation experiments with dsDNA. BPES buffer [BPE buffer containing additional 185 mM NaCl (pH 7.0)] was used for thermal denaturation studies with triplex DNA.

Nucleic Acids. Calf thymus DNA (ctDNA, type I, highly polymerized sodium salt) and salmon testes DNA were purchased from Sigma (St. Louis, MO). They were dissolved in an appropriate buffer at a concentration of 1−2 mg/mL and left at 4 °C overnight. After being treated (10 min) in an ultrasonic bath, the solution was filtered through a PVDF membrane filter (pore size of 0.45 μm) to remove any insoluble material. Polynucleotides $[poly(dAdT)]_2$, $[poly(dGdC)]_2$, poly(dA)-poly(dT), and poly(dT) were purchased from Amersham Biosciences (Piscataway, NJ) and used without further purification or treatment. Triplex poly(dA)-$[poly(dT)]_2$ was prepared by mixing equimolar amounts of poly(dT) and poly(dA)-poly(dT), each dissolved in BPES buffer at a concentration of approximately 1 mM (bases and base pairs, respectively), heating the mixture to 90 °C in a water bath, and slowly cooling it to 4 °C overnight. Concentrations of nucleic acid samples were determined by UV absorbance measurements of a diluted (1:20) stock solution, using the published values of the extinction coefficients (*28*). The quality of nucleic acids samples was

checked by comparing their melting temperatures with the published data at identical buffer compositions (*28*, *29*). If not stated otherwise, the DNA concentrations are expressed in nucleobase units.

Spectrophotometric titrations were performed according to the established protocols in ETN buffer at 25 °C (*30*). The hypochromicity H of the ligands upon binding to DNA was calculated with the equation $H = 1 - E_{DNA}/E_0$, where E_0 and E_{DNA} are the integrated extinction coefficients of the free ligand and of the ligand−DNA complex in the long-wavelength range (300−500 nm), respectively (*31*).

Linear and Circular Dichroism Spectroscopy. Linear dichroism spectra of the ligand−nucleic acid complexes were recorded in ETN buffer in a flow cell on a Jasco J500A spectropolarimeter equipped with an IBM PC and a Jasco J interface. Partial alignment of the DNA was provided by a Wada−Kozawa linear-flow device (*32*) at a shear gradient of approximately 800 rpm. The concentration of DNA in samples for LD spectroscopy was 2.27 mM, and ligand-to-DNA ratios (r) of 0, 0.04, 0.08, and 0.2 were used. Data evaluation and determination of binding geometry were performed as described previously (*33*, *34*). The CD spectra were recorded at a DNA concentration of 30 μM and ligand-to-DNA ratios of 0, 0.04, 0.2, and 0.4 on a Jasco J800 apparatus. The spectra presented here represent results of four averaged scans.

Viscosimetry of DNA Solutions. Viscosimetric measurements were performed in a micro-Ubbelohde capillary viscosimeter thermostated at 25.0 °C. The viscosimeter was filled with 2.5 mL of a 1 mM (bp) solution of sonicated ctDNA (Trevigen, Gaithersburg, MD; average length of 200 bp) in BPE buffer. The aliquots (5−20 μL) of the solution of the ligand in the same buffer (5 mM) were added by means of a microsyringe, until the final concentration of the ligand in the viscosimeter reached 0.2 mM. After each addition, the sample was thoroughly mixed by bubbling air through the liquid and equilibrated for several minutes, and the flow times were determined in triplicate.

The specific viscosity of the DNA solutions was calculated with the equation $\eta = (t - t_0)/t_0$, where t_0 is the flow time of the buffer solution and t is the flow time of the DNA solution. The $(\eta/\eta_0)^{1/3}$ values, where η_0 and η are the relative viscosities of the DNA solutions in the absence and presence of varied concentrations of ligand, respectively, were plotted versus the ligand-to-DNA ratio (r).

DNA thermal denaturation studies were performed according to the established protocols (*27*), using BPE buffer for dsDNA and BPES buffer for triplex DNA poly(dA)-[poly(dT)]$_2$. The samples were heated from 20.0 to 97.0 °C at a rate of 0.2 °C/min, while the absorbance was monitored at 260 nm. The melting temperatures (T_m) were determined from the first-order derivatives of melting curves.

Computational Methodologies. All modeling studies were carried out on a 12-CPU cluster running under openMosix architecture. The structures of diazoniapolycyclic cations were optimized using Hartree−Fock calculations with the 6-311++G(d,p) basis set. The quantum chemistry calculations were carried out with Gaussian 98 (*35*). Harmonic vibrational frequencies were obtained from RHF/6-311++G-(d,p) calculations and used to characterize local energy minima (all frequency real). Atomic charges were calculated by fitting to the electrostatic potential maps (CHELPG method) (*36*).

(1) Duplex Intercalation Site Preparation. This study involved the use of consensus dinucleotide intercalation geometries d(ApT) and d(GpC) initially obtained using NAMOT2 (Nucleic Acid MOdeling Tool, Los Alamos National Laboratory, Los Alamos, NM) (*37*). The d(ApT) and d(GpC) intercalation sites were contained in the center of a decanucleotide duplex of sequences d(5′-ATATA-3′)$_2$ and d(5′-GCGCG-3′)$_2$, respectively. The decamers in the B-form were built using the "DNA Builder" module of Molecular Operation Environment (MOE, version 2005.06) (*38*). The decanucleotides were minimized using the Amber94 all-atom force field (*39*) implemented by MOE, until the root-mean-square (rms) value of the Truncated Newton method (TN) was <0.1 kcal mol^{-1} Å^{-1}. To model the effects of solvent more directly, a set of electrostatic interaction corrections was used. The MOE suite implemented a modified version of the GB/SA contact function described by Still and co-workers (*40*). These terms simulate the electrostatic contribution to the free energy of solvation in a continuum solvent model.

(2) Molecular Docking Protocol. Diazoniapolycyclic salts were docked into both intercalation sites using the flexible MOE-Dock methodology. The purpose of MOE-Dock is to search for favorable binding configurations between a small, flexible ligand and a rigid macromolecular target. Searching is conducted within a user-specified three-dimensional docking box, using the "tabù search" protocol (*41*) and MMFF94 force field (*42*). Charges for diazoniapolycyclic salts were imported from the Gaussian output files. MOE-Dock performs a user-specified number of independent docking runs (55 in the presented case) and writes the resulting conformations and their energies to a molecular database file. The resulting DNA−diazoniapolycyclic salt complexes were subjected to MMFF94 all-atom energy minimization until the rms value of the conjugate gradient was <0.1 kcal mol^{-1} Å^{-1}. GB/SA approximation has been used to model the electrostatic contribution to the free energy of solvation in a continuum solvent model.

(3) Binding Free Energy Calculation. The binding free energies were calculated using the MM-GBSA free energy calculation method (*43*). In this method, the free energy of inhibitor binding, ΔG_{bind}, is obtained from the difference between the free energy of the receptor−ligand complex (G_{cpx}) and the unbound receptor (G_{rec}) and ligand (G_{lig}) according to the following equation:

$$\Delta G_{bind} = G_{cpx} - (G_{rec} + G_{lig})$$

The binding free energy (ΔG_{bind}) was evaluated in four DNA−molecule complexes obtained as docking results. ΔG_{bind} was calculated as a sum of changes in the energy of three different contributions: (i) a force field term (E_{FF}) for bond, angle, torsional, van der Waals, and electrostatic potential energies, (ii) a polar solvation free energy part (ΔG_{GB}), calculated according to the generalized Born approximation model (*44*), and (iii) a nonpolar contribution to the solvation free energy (ΔG_{NP}):

$$\Delta G_{bind} = E_{FF} + \Delta G_{GB} + \Delta G_{NP}$$

$$\Delta G_{NP} = \gamma \times SASA$$

where SASA represents the solvent accessible surface area of the solute while γ is an empirical parameter (0.005 kcal mol^{-1} Å^2).

(4) Determination of the Transition Dipole Moments. The transition dipole moments were calculated using the semiempirical AM1 Hamiltonian and the configuration-interaction method implemented in HyperChem (*45*) employing the energy-minimized ground-state geometry. The CI calculations involved the five highest occupied and five lowest unoccupied molecular orbitals and a total of 51 singly excited configurations.

RESULTS

Binding of DAPS to Double-Stranded DNA

Spectrophotometric Titrations. The interaction of DAPS with DNA was monitored by spectrophotometric titrations of their solutions in an aqueous buffer with salmon testes DNA (stDNA). Representative spectrophotometric titrations are shown in Figure 1 (for the corresponding graphs of the other derivatives, see Figure S1 of the Supporting Information). Along with a significant hypochromism (20−30%) and a partial loss of the fine structure of absorption bands, the absorption maxima of most DAPS exhibit bathochromic shifts of 5−10 nm upon formation of a complex with DNA, relative to the free ligands (Table 1). Moreover, several isosbestic points were detected in each case. In the case of the spectrophotometric titration of DNA to diazoniahexaphene **6**, hypochromism and red shifts of absorption maxima were observed (Figure 1); however, an isosbestic point was maintained only at the end of the titration, i.e., at DNA-to-ligand ratios of >1.3, whereas at lower concentrations of DNA, no isosbestic point was observed. Finally, the addition of the DNA resulted in an only minor hypochromic effect in the case of derivative **7** (not shown).

The binding isotherms, derived from the spectrophotometric titrations, were represented as Scatchard plots, which were analyzed according to the model of McGhee and von Hippel (*30*, *46*) to estimate the apparent association constant (*K*) and the number of base pairs (*n*) covered by the ligand molecules upon binding to the DNA (Table 1). The binding site sizes were in the 2.0−2.5 bp range for all DAPS; at the same time, the values of the binding constants depend on the structure of DAPS. Diazoniapentaphenes **4a**−**e** have similar binding constants (1−2 × 10^5 M^{-1}), whereas the hexacyclic derivatives have significantly higher DNA affinity (∼5 × 10^6 M^{-1} for **5b** and **5c**). In the case of compound **6**, the apparent binding constant (∼5 × 10^5 M^{-1}) is actually a combination of at least two binding constants, as the photometric DNA titration indicates more than one binding mode, and the two binding constants could not be resolved from the available data.

Linear Dichroism Spectroscopy. We used LD spectroscopy to evaluate the binding modes between ligands **4a**−**e**, **5a**−**c**, **6**, and **7** and DNA, with the DNA molecules being oriented in a hydrodynamic field (flow linear dichroism) (*33*, *34*). Except for compound **7**, the LD signals of complexes of DNA with DAPS are negative at different ligand-to-DNA ratios (0.04, 0.08, and 0.20) both in the UV region, where the DNA and the ligands absorb, and at longer wavelengths,

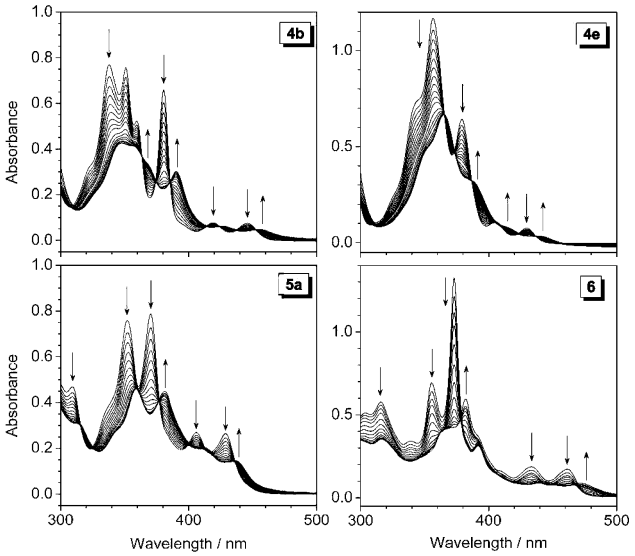

FIGURE 1: Spectrophotometric titrations of stDNA (0−0.1 mM) to compounds **4b**, **4e**, **5a**, and **6** at a ligand concentration of 20 μM. Arrows indicate the changes of the intensity of the absorption bands upon addition of DNA.

Table 1: DNA Binding Constants (*K*) and Binding Site Sizes (*n*) of Diazoniapolycyclic Ions **4**−**6** Determined from Spectrophotometric Titrations[a]

ligand	*H* (%)[b]	*K* (×10^5 M^{-1})[c]	*n* (bp)[d]
4a	43[e]	5.7[e]	2.8[e]
4b	21	1.8	2.0
4c	28	1.2	2.5
4d	20	1.8	2.5
4e	29	1.8	2.5
5a	19	6.4	2.0
5b	28	46.1	2.0
5c	20	50.2	2.2
6	27	4.9	0.9
7	2.5	nd[f]	nd[f]

[a] Experimental conditions: ETN buffer [10 mM TRIS, 1 mM EDTA, and 10 mM NaCl (pH 7.0)] at 25 °C. [b] Hypochromicity (in the 300−500 nm range) of the ligands upon formation of a complex with DNA. [c] Apparent binding constants. [d] Binding site sizes (in base pairs), calculated from fitting of the binding isotherms to the McGhee−von Hippel model. [e] From ref *26* and from spectrofluorimetric titrations. [f] Not determined.

where only the ligands absorb (Figure 2, top panels). The negative LD signals in the long-wavelength regions (300−450 nm) indicate that the transition dipole moments and thus the π-systems of ligands **4a**−**e**, **5a**−**c**, and **6** are coplanar to the ones of the nucleic bases upon binding to the DNA. The addition of the ligands also leads to a significant increase in the magnitude of the LD signal of the absorption band of the DNA bases (≈260 nm), which usually reveals stiffening of the DNA molecule and a better orientation of the DNA molecules along the flow lines.

In the case of compound **7**, only a weak LD signal in the region of the ligand absorption (300−420 nm) was observed in the presence of DNA. Interestingly, the LD signal of **7** is negative at low ligand-to-DNA ratios but becomes bisignate at higher ligand loading [$r = 0.20$ (Figure 5I)]. At the same time, the addition of this compound to the DNA results in a moderate decrease in the magnitude of the LD signal of the DNA bases, which indicates an interaction between dsDNA and **7**.

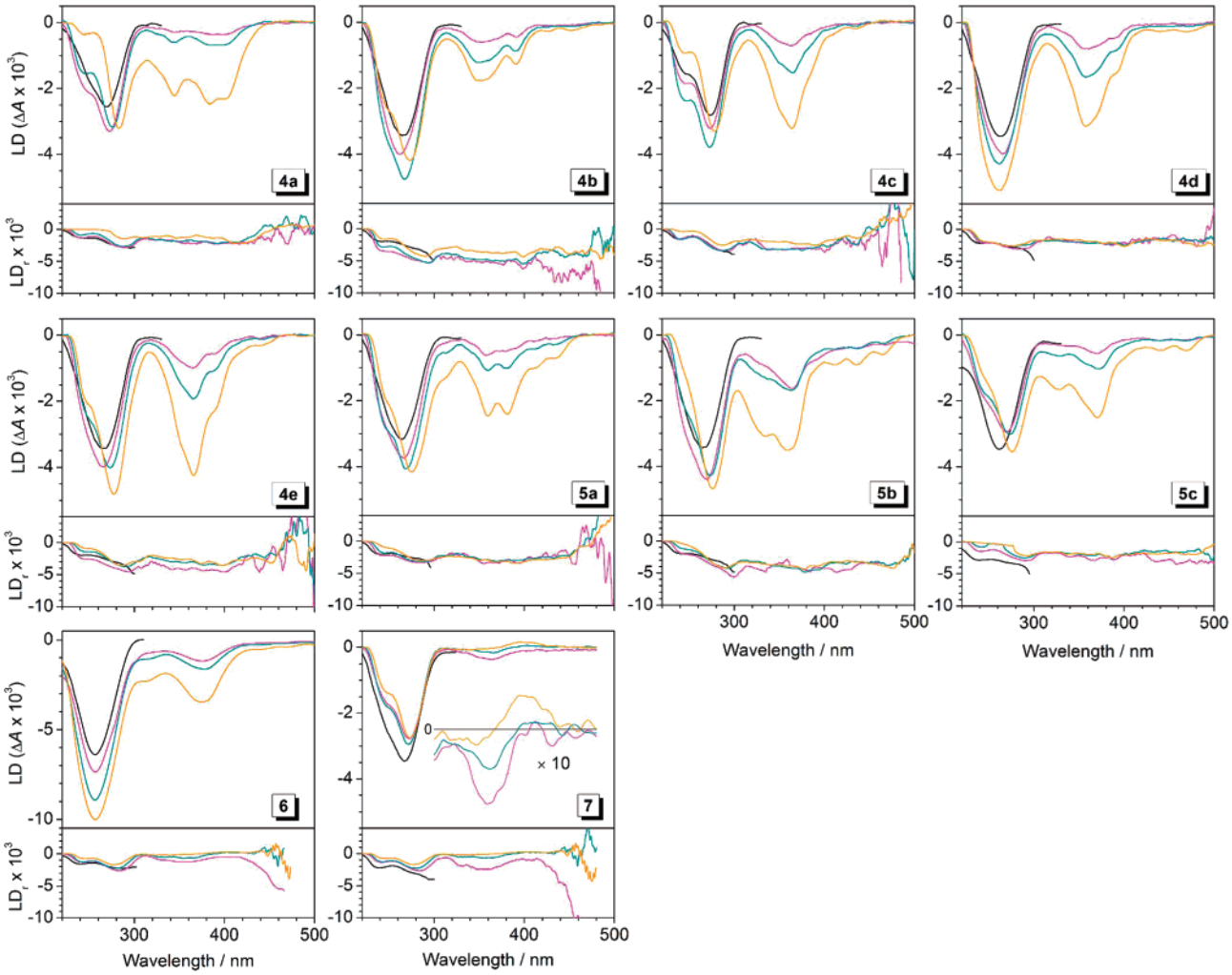

FIGURE 2: Linear dichroism (LD, top panels) and reduced LD (LD_r, bottom panels) spectra of compounds **4a**−**e**, **5a**−**c**, **6**, and **7** in the presence of stDNA (2.27 mM, in bases) at different ligand-to-DNA ratios (black for $r = 0$, magenta for $r = 0.04$, green for $r = 0.08$, and orange for $r = 0.20$); the more intense LD signals of DNA and ligand **6** result from a new setup in this particular experiment, which allows better orientation of the DNA in the flow cuvette.

The reduced LD spectra [$LD_r = LD/A_{iso}$ (Figure 2, bottom panels)] of DNA−ligand complexes provide further information about the average orientation of the transition moment of the dye relative to those of the DNA bases and allow us to distinguish between homogeneous and heterogeneous binding. Except for those of compound **7**, almost constant LD_r spectra over the range of 310−400 nm were observed, indicating an almost exclusive intercalation of DAPS into dsDNA. In the regions where $\lambda > 420$ nm, a significant fluctuation of the LD_r signal was observed because of the low absorbance of the ligands at these wavelengths.

Circular Dichroism Spectroscopy. In the case of DAPS **4b**−**e** and **5a**−**c**, the CD spectra of stDNA exhibit a moderate increase in the magnitude of the positive CD signal of DNA (275 nm) in the presence of increasing concentrations of DAPS (Figure 3). Additionally, induced CD (ICD) signals are observed in the regions of the absorption of the ligands (300−450 nm), which are usually negative (−0.2 to −1.8 mdeg at $c_{DNA} = 30\ \mu M$); however, in the case of diazoniapentaphene **4a**, a weak positive ICD was observed [1.3 mdeg at $r = 0.4$ (Figure 3)]. In the cases of **4e** and **5b**, the ICD signals of the ligands were bisignate and additional weak positive ICD bands were observed, which are indicative of the exciton interactions between the bound ligands (*34*).

The CD spectra of complexes of diazoniahexaphene **6** with DNA reveal a bathochromic shift of the positive CD signal of the DNA (Figure 3), and an isoelliptic point at 280 nm was observed. In contrast to DAPS **4b**−**e**, **5a**, and **5b**, which exhibit moderate negative ICD signals, diazoniahexaphene **6** shows a strong (8 mdeg at $r = 0.2$), well-resolved positive ICD signal in the region of 330−450 nm. Finally, addition of compound **7** to DNA does not lead to significant changes in the CD spectrum of stDNA, whereas a weak positive ICD signal (0.2 mdeg) of the ligand was observed in the long-wavelength region (Figure 3).

Viscosimetric Titrations. The interaction of the ligands with DNA has an effect on the hydrodynamic properties of the solutions of the biopolymers (*47*). At low ligand-to-DNA ratios ($r < 0.2$), the intercalation of the ligands between the DNA base pairs leads to the elongation of the biomacromolecule and increases the viscosity of the solution. In the case of ethidium bromide, which was chosen as a reference compound, a linear dependence of the cubic root of the relative viscosity on the ligand-to-DNA ratio was observed (Figure 4) with a slope k of 0.92, which is consistent with literature data (*48*). The diazoniapentaphene **4c** and diazoniaanthra[1,2-*a*]anthracene **5a** behave similarly, leading to an increase in the viscosity of the DNA solutions, albeit with

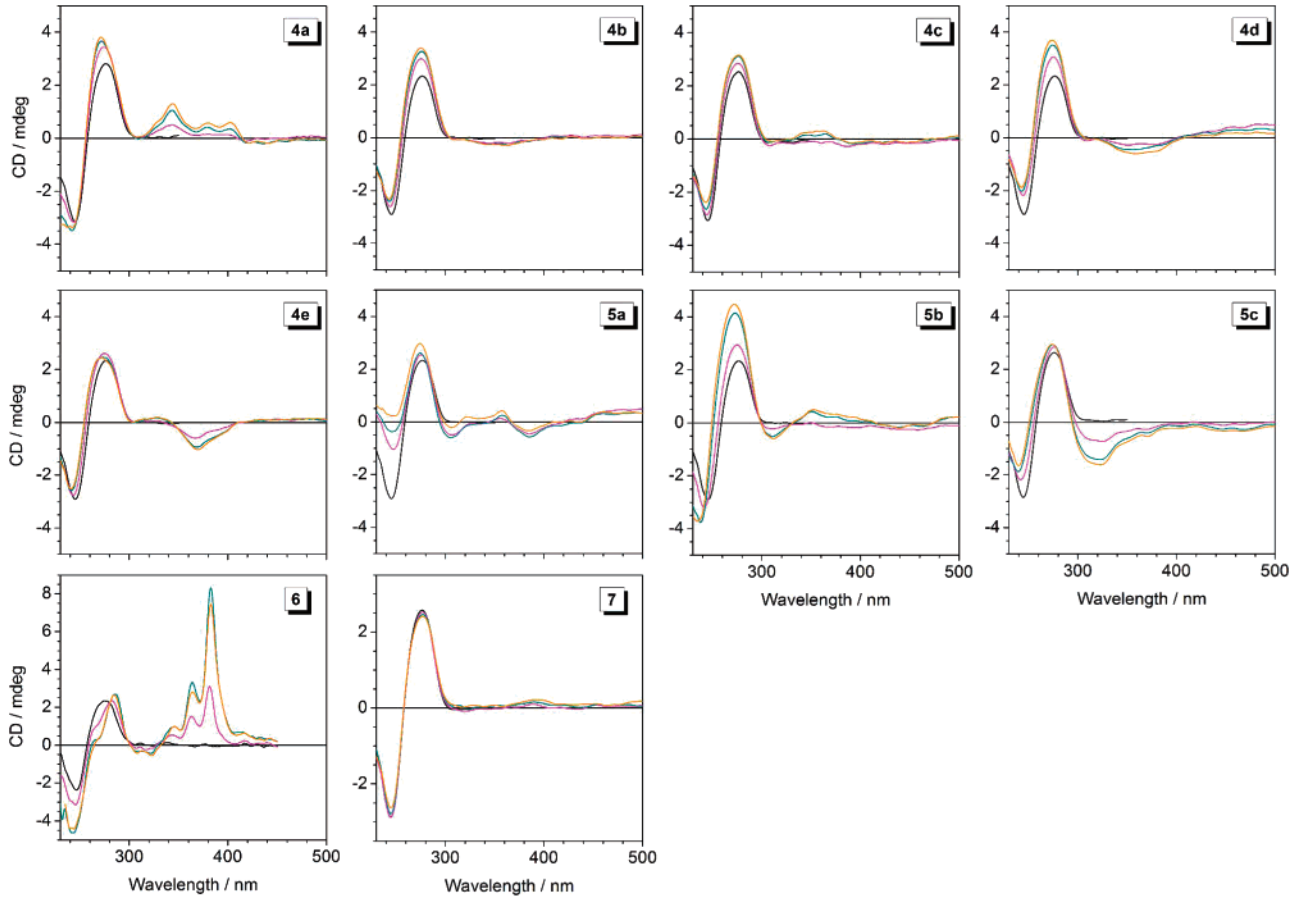

FIGURE 3: CD spectra of compounds **4a**−**e**, **5a**−**c**, **6**, and **7** in the presence of stDNA (30 μM in bases) at different ligand-to-DNA ratios (black for $r = 0$, magenta for $r = 0.04$, green for $r = 0.20$, and orange for $r = 0.40$). Note the different scale in the case of compounds **6** and **7**.

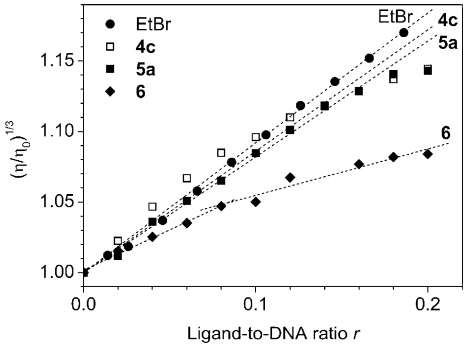

FIGURE 4: Effect of ethidium bromide and DAPS **4c**, **5a**, and **6** on the relative viscosity of a solution of ctDNA (1 mM bp in BPE buffer) at 25 °C. The dotted lines represent linear fits of experimental data.

slightly smaller slopes (0.86 and 0.82, respectively). At the same time, the increase in the viscosity seems to reach saturation at lower r values as compared to ethidium. Notably, the addition of diazoniahexaphene **6** leads to a much less pronounced increase in the viscosity of DNA solutions ($k = 0.57$ at $r < 0.1$ and $k = 0.33$ at $r \geq 0.1$).

DNA Thermal Denaturation Studies. The DNA binding properties of diazoniapolycyclic ions were studied by thermal denaturation experiments with two types of dsDNA, calf thymus DNA (ctDNA, 42% GC) and an alternating polynucleotide [poly(dAdT)]$_2$. The stabilizing effect of the ligands was investigated under incomplete saturation conditions, i.e., at ligand-to-DNA ratios (r) of 0.2 and 0.5, and at low ionic strengths of buffer (BPE buffer) so that the melting transitions could be observed at moderate temperatures, and to allow a direct comparison with other known DNA ligands (*29*). Proflavine (3,6-diaminoacridine), an intercalator whose DNA binding properties are well-documented (*49*−*51*), and the parent system, the acridizinium ion (**1**), were used as reference compounds. The ΔT_m values for the diazoniapolycyclic salts are presented in Table 2. For two representative

Table 2: DNA Binding Properties of Ligands from Thermal Denaturation Studies[a]

	induced ΔT_m (°C)				
	ctDNA		[poly(dAdT)]$_2$		
ligand	$r = 0.2$	$r = 0.5$	$r = 0.2$	$r = 0.5$	base selectivity[b]
proflavine	10.1 (11.5[c])	15.6	18.4	24.0	AT
1	1.2 (2[d])	2.6 (3[d])	1.6 (2[d])	3.5 (4[d])	AT
4a	12.1	19.0	11.3	16.2	GC
4b	11.8	17.5	8.5	15.4	GC
4c	12.1	17.6	8.4	15.2	GC
4d	13.0	20.5	10.0	17.0	GC
4e	12.6	18.1	8.3	14.9	GC
5a	15.4	30.2	13.3[e]	23.3	GC
5b	16.7	30.4	19.6[e]	32.8	AT
5c	18.7	28.6	18.8[e]	28.7	none
6	15.1	21.7	25.4	35.0	AT
7[f]	2.0	5.8	3.4	7.4	AT

[a] Experimental conditions: $c_{DNA} = 40$ μM (bp) in BPE buffer, $[Na^+] = 16$ mM; estimated error of ±0.2 °C. [b] Based on comparison of ΔT_m(ctDNA) and ΔT_m[poly(dAdT)$_2$] values. [c] From ref *29*. [d] From ref *19*. [e] Biphasic curve, T_m determined from the midpoint of the transition. [f] Thermal decomposition of the ligand was observed at temperatures of >70 °C but did not influence the T_m determinations.

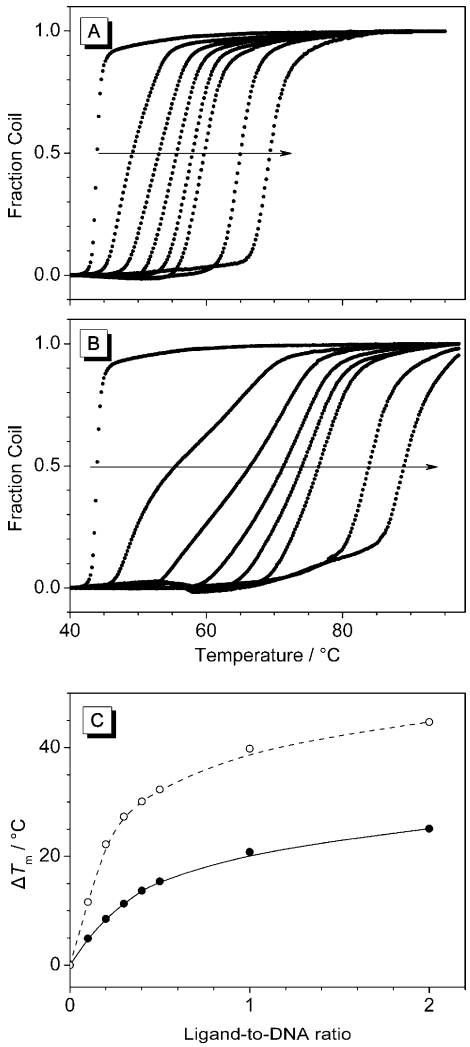

FIGURE 5: (A and B) Thermal denaturation profiles of [poly(dAdT)]$_2$ duplex (c_{DNA} = 40 μM bp in BPE buffer) in the presence of **4b** (A) and **5b** (B) at ligand-to-DNA ratios (*r*) of 0, 0.1, 0.2, 0.3, 0.4, 0.5, 1.0, and 2.0. Arrows indicate the shift of the melting curves with increasing *r* values. (C) Plot of ligand-induced T_m shifts vs ligand-to-DNA ratio.

ligands, diazoniapentaphene **4b** and diazoniaanthra[1,2-*a*]anthracene **5b**, the influence of the ligand-to-DNA ratios on the DNA melting profiles was studied over a broader range (0.1−2.0) of *r* values (Figure 5).

At low ionic strengths, all diazoniapolycyclic salts, except for derivative **7**, stabilize the double-stranded DNA with respect to thermal denaturation to a very large extent. That is, the diazoniapentaphenes **4a**−**e** increase the temperatures of the helix−coil transition of ctDNA by 18−20 °C (ΔT_m) at r = 0.5. This stabilization is much more pronounced than the one induced by the monocationic acridizinium ion **1** (ΔT_m = 2.6 °C) and is comparable to the one induced by proflavine (ΔT_m = 15.6 °C). Especially large effects are observed for diazoniaanthra[1,2-*a*]anthracenes **5a**−**c** ($\Delta T_m \approx$ 30 °C at r = 0.5). Although thermal denaturation experiments with the [poly(dGdC)]$_2$ duplex were not possible under the conditions that were employed (T_m > 100 °C), a comparison of ΔT_m values observed with ctDNA (42% GC) and those obtained with [poly(dAdT)]$_2$ allowed us to evaluate the base selectivity of the ligands. Thus, most diazoniapolycyclic salts exhibit a slightly larger stabilization of ctDNA compared to the [poly(dAdT)]$_2$ duplex, presumably due to the preferential binding

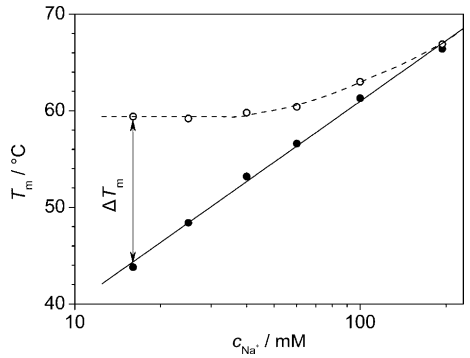

FIGURE 6: Influence of the total Na^+ concentration on the T_m transitions of [poly(dAdT)]$_2$ in the absence (●) and presence of **4b** (○) at a ligand-to-DNA ratio of 0.5.

to GC-rich DNA regions. However, compounds **5b** and **6** display preferential high-affinity binding to [poly(dAdT)]$_2$. The diazoniahexaphene **6** shows an exceptionally strong stabilization of [poly(dAdT)]$_2$ (ΔT_m = 35 °C at r = 0.5), while its binding to ctDNA is less pronounced.

In contrast, derivative **7** has much weaker effects on the melting transition of DNA. The induced T_m shifts (ΔT_m = 5−7 °C at r = 0.5) are in the range which is characteristic for weak DNA binders, such as acridizinium **1** and the unsubstituted acridine (*29*), and a slight preference for AT-rich DNA is observed. Moreover, a drift in the DNA melting profiles is induced by this compound, which we attribute to its partial thermal decomposition. For these reasons, this compound was excluded from the further DNA binding studies.

Dependence of Melting Temperatures on Ionic Strength. Because the thermal denaturation experiments with triplex DNA needed to be performed at ionic strengths higher than those used for the dsDNA due to the instability of the triplex at low ionic strengths (in the absence of divalent cations or polyamines), we first examined the influence of the salt concentration on the melting behavior of dsDNA in the presence of selected DAPS ligands. It is known that the ΔT_m values, obtained under different ionic strength conditions, cannot be directly used for comparison of the binding affinities of the ligands for DNA, since the melting temperature of DNA depends strongly on the salt concentration even in the absence of ligands (*52*). On the other hand, binding of the ligands to the DNA also depends on the salt concentration, due to the competition between the positively charged ligands and the monovalent salt cations for available DNA binding sites, as well as on the overall charge of the ligand (*53*). This dependence is complicated and cannot be analyzed completely in the absence of the thermodynamic parameters (enthalpy of binding) obtained by independent methods. Moreover, in this work, mainly subsaturating ligand concentrations were used, which allow a better comparison between different ligands but cannot be analyzed, with respect to the binding thermodynamics, by the established methods (*54*, *55*). For these reasons, the influence of the salt concentration on the melting behavior of DNA was evaluated empirically by the measurements of T_m values of the double-stranded polynucleotide, [poly(dAdT)]$_2$, in the presence and absence of a representative ligand **4b** at the same concentrations, but under various ionic strength conditions (Figure 6).

The melting temperature of the [poly(dAdT)]$_2$ duplex in the absence of the ligand is linearly dependent on log[Na^+]

in the range of salt concentrations between 16 and 200 mM, as characterized by the empirical Schildkraut−Lifson equation (*52*, *56*). In the presence of subsaturating amounts of ligand, the T_m expresses a complex behavior; that is, at low Na^+ concentrations ($[Na^+] \leq 50$ mM), the melting temperature of the ligand−DNA complex is almost independent of the salt concentration. With an increasing salt concentration, the melting temperatures asymptotically approach the ones that are observed in the absence of the ligand. At these salt concentrations, the binding constant of a ligand is reduced to a level that does not significantly contribute to the binding and stabilization of the double helix. It should be emphasized that the salt influence is especially important for the diazoniapolycyclic ligands, as these are doubly positively charged species.

Binding of Diazoniapolycyclic Ions to Triple-Helical DNA

DNA Thermal Denaturation Studies. Thermal denaturation experiments were used to investigate the binding of diazoniapolycycles to triple-helical DNA, namely the poly(dA)-$[poly(dT)]_2$ triplex, which is readily prepared from poly(dA)-poly(dT) and poly(dT) and is stable at neutral pH values. As in reported protocols (*28*), thermal denaturation studies with triplex DNA were performed under the conditions of relatively high ionic strength ($[Na^+] = 200$ mM), to eliminate the interference of otherwise used buffer components, such as polyvalent metal cations (Mg^{2+}) or polyamines, which may also stabilize the triplex (*57*). Under these conditions, the melting profiles of the poly(dA)-$[poly(dT)]_2$ triplex are biphasic: when $T_m^{3\rightarrow2} = 42.8$ °C, the triplex dissociates into the poly(dA)-poly(dT) duplex and a single-stranded poly(dT) (Hoogsten transition), whereas when $T_m^{2\rightarrow1} = 74.8$ °C, the remaining double helix dissociates (Watson−Crick transition). The diazoniapolycyclic ions have a pronounced influence on the melting behavior of the triplex DNA (Figure 7). Thus, at low ligand-to-DNA ratios ($r \leq 0.5$), diazoniapentaphenes **4a**−**e** induce large shifts of the triplex-to-duplex transition to higher temperatures [$\Delta T_m^{3\rightarrow2} = 14-17$ °C at $r = 0.5$ (Table 3)]. At the same time, the temperature of the duplex denaturation is only slightly affected ($\Delta T_m^{2\rightarrow1} = 0.7-1.3$ °C). These observations show that, under the conditions that were employed, salts **4a**−**e** are capable of selective binding to and stabilization of the triple-helical DNA. It should be noted that at the high ionic strengths used in these experiments, in contrast to the melting experiments with double-stranded DNA which were performed at lower ionic strengths (16 mM Na^+; see Table 2), the interaction of the ligands with DNA is suppressed to such an extent that it almost does not lead to a thermodynamic stabilization of the duplex DNA, whereas the stabilization of the less thermodynamically stable triplex motif becomes prominent.

Compared to derivatives **4a**−**e**, diazoniaanthra[1,2-*a*]anthracenes **5a**−**c** have an even more pronounced influence on the thermal stability of the triple-helical DNA. Thus, at ligand-to-DNA ratios of 0.5, these compounds increase the temperature of the Hoogsten transition ($\Delta T_m^{3\rightarrow2}$) by ≈30 °C; in the case of **5a**, the two melting transitions merge almost completely at $r \geq 0.3$. However, these ligands also induce more severe shifts of the temperature of the duplex-to-coil transitions. This effect is most pronounced in the case of **5b** and **5c** ($\Delta T_m^{2\rightarrow1} \approx 9-10$ °C at $r = 0.5$), indicating that these compounds have lower triplex-versus-duplex selectivity. The isomer **5a** shows an exceptionally high selectivity at low r values; that is, at $r = 0.2$, the induced $T_m^{3\rightarrow2}$ shift is 26 °C and thus far larger than those observed with diazoniapentaphenes **4a**−**e**, whereas the $\Delta T_m^{2\rightarrow1}$ is only 0.7 °C.

Notably, diazoniahexaphene **6** has the lowest triplex-versus-duplex selectivity among the investigated DAPS. Thus, this compound stabilizes the triplex DNA to a lesser extent than diazoniapentaphenes and diazoniaanthra[1,2-*a*]anthracenes ($\Delta T_m^{3\rightarrow2} = 12.9$ °C vs 14−17 °C for compounds

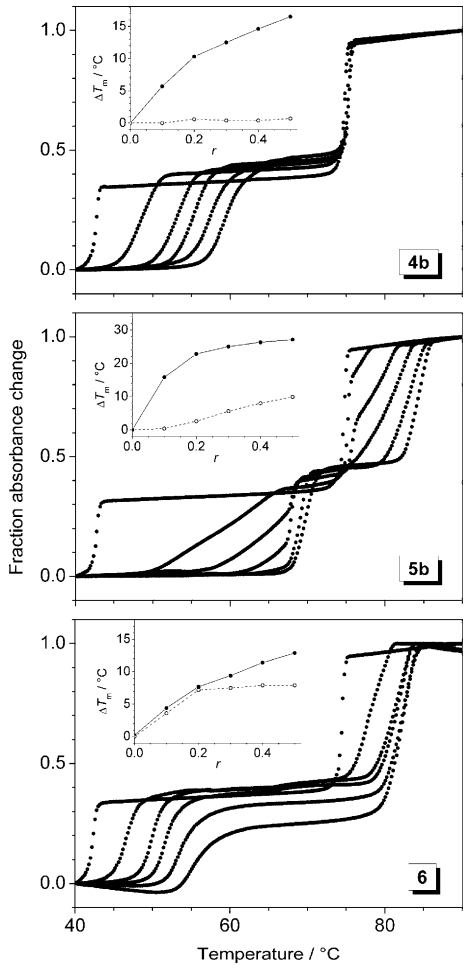

FIGURE 7: Melting profiles of poly(dA)-$[poly(dT)]_2$ in the presence of DAPS **4b**, **5b**, and **6** at ligand-to-DNA ratios (r) of 0, 0.1, 0.2, 0.3, 0.4, and 0.5; $c_{DNA} = 40$ μM (base triplets) in BPES buffer. Insets show the dependence of T_m shifts [$\Delta T_m^{3\rightarrow2}$ (●) and $\Delta T_m^{2\rightarrow1}$ (○)] on the ligand-to-DNA ratio.

Table 3: Stabilization of the Poly(dA)-$[Poly(dT)]_2$ Triplex by DAPS As Determined by Thermal Denaturation Studies[a]

	$r = 0.2$		$r = 0.5$	
ligand	$\Delta T_m^{3\rightarrow2}$	$\Delta T_m^{2\rightarrow1}$	$\Delta T_m^{3\rightarrow2}$	$\Delta T_m^{2\rightarrow1}$
proflavine	4.5	0.4	6.6	1.3
4a	11.3	1.0	17.1	1.3
4b	10.3	0.6	16.5	0.7
4c	11.3	0.5	17.5	0.9
4d	11.6	0.8	17.4	0.9
4e	8.6	0.6	13.7	0.7
5a	26.3	0.7	34.1	5.8
5b	22.8	2.6	27.1	9.9
5c	27.7	3.6	31.6	10.2
6	7.7	7.2	12.9	7.9

[a] Experimental conditions: $c_{DNA} = 40$ μM (base triplets) in BPES buffer, $[Na^+] = 200$ mM; estimated error in T_m determinations of ±0.2 °C.

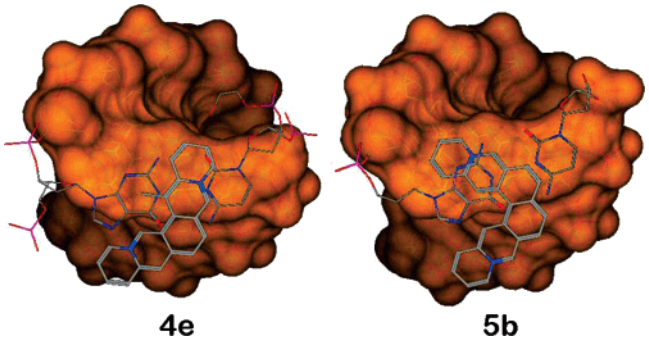

FIGURE 8: Molecular models of diazoniapentaphene **4e** (left) and diazoniaanthra[1,2-*a*]anthracene **5b** (right) intercalated into the [poly(dGdC)]$_2$ duplex (see Experimental Procedures for details); dsDNA is represented by its Connolly's surface.

4a−**e** at $r = 0.5$). At the same time, the temperature of the duplex denaturation is increased significantly ($\Delta T_m^{2\rightarrow1} =$ 7.9 °C at $r = 0.5$), indicating a strong preference for the duplex form of DNA in this case.

Molecular Modeling Studies

To further assess the structure of the ligand−DNA complex, molecular modeling investigations were performed with diazoniapentaphene **4e** and diazoniaanthra[1,2-*a*]anthracene **5b**. These calculations show that the intercalation of these ligands into DNA is an exergonic process. In Figure 8, the best docking pose of compounds **4e** (panel A) and **5b** (panel B) intercalated into the [poly(dGdC)]$_2$ duplex is shown (cf. Supporting Information for presentation with 90° rotation). As compared to diazoniapentaphene derivative **4e**, diazoniaanthra[1,2-*a*]anthracene **5b** provides a relatively large overlap area between the intercalator and the two DNA base pairs that constitute the intercalation pocket; i.e., one azoniaanthracene part of **5b** is accommodated in the intercalation site with the other azoniaanthracene moiety pointing inside the DNA groove. Indeed, the theoretical energies of intercalation support the idea that **5b** is more effective as an intercalator than derivative **4e** in both AT and GC intercalation sites (AT site, $\Delta G_{bind-5b} = -17.1$ kcal/mol vs $\Delta G_{bind-4e} = -10.2$ kcal/mol; GC site, $\Delta G_{bind-5b} = -16.8$ kcal/mol vs $\Delta G_{bind-4e} = -9.8$ kcal/mol).

DISCUSSION

Binding of DAPS to the Double-Stranded DNA

Mode of Binding to the Duplex DNA. The diazoniapolycyclic salts, which were investigated in this study, are cationic polyaromatic compounds that are planar structures (**4a**−**c** and **6**) or have some degree of tilting (**4d,e**, **5a**−**c**, and **7**). These structural properties of DAPS have been determined by the X-ray structural analysis of the representative derivatives (*22*, *25*).

The interaction with dsDNA leads to significant changes in the absorption spectra of all DAPS, providing evidence of the binding. The presence of the isosbestic points, observed in most cases, indicates that the changes in the absorption spectra are due to two states of the chromophore, namely, the free and bound ligands. Moreover, since the isosbestic points are conserved over a wide range of ligand-to-DNA ratios, it may be concluded that one binding mode is adopted almost exclusively. In contrast, during titration of DNA to compound **6**, an isosbestic point is not conserved, an indication of significant heterogeneous binding. The absorption of all the ligands, except for **7**, is significantly reduced (hypochromism value of 20−30%) in the presence of DNA, which indicates a strong electronic interaction between the π-electrons of the ligands and those of nucleic bases. For comparison, the large hypochromism is characteristic of the anthracene derivatives which are intercalated into the DNA (*11*).

The linear dichroism data provide further information about the mode of binding of DAPS to dsDNA, namely, the orientation of the chromophore of the ligands bound to the DNA helix. Thus, intercalation of the aromatic ligands, such as anthracene and acridine derivatives, results in a perpendicular orientation of the chromophore plane and transition dipole moments with respect to the DNA helix axis (i.e., coplanar with the nucleic bases), which gives rise to negative LD signals of the bound ligands, such as the ones of the nucleic bases that have the same relative orientation of the π-system. At the same time, the ligands bound in the DNA grooves are oriented with an angle of approximately 45°, which results in positive LD signals.

Diazoniapentaphenes **4b**−**e**, diazoniaanthra[1,2-*a*]anthracenes **5a**−**c**, and diazoniahexaphene **6** exhibit negative induced LD signals in the presence of DNA, which are indicative of the intercalative binding mode, as reported previously for compound **4a** (*26*). At the same time, the reduced LD spectra are nearly constant in the region of the absorption of the ligands at all ligand-to-DNA ratios, which confirms that one binding mode is adopted exclusively under these conditions. Thus, the LD spectroscopic analysis of the ligand−DNA complexes clearly demonstrates that the diazoniapolycyclic derivatives **4** and **5** intercalate into DNA. These observations are fully consistent with the viscosimetric studies, because the latter revealed an influence of ligands **4** and **5** on the viscosity of the DNA solution which is characteristic of intercalators, as demonstrated by comparison with ethidium bromide. In contrast, diazoniahexaphene **6** appears to have much less influence on the viscosity of the DNA solutions, which may indicate an at least partial contribution of the groove binding mode. Notably, this observation is inconsistent with the LD spectroscopic experiments which show that **6** exclusively intercalates at ligand-to-DNA ratios up to 0.2. However, a detailed inspection of the change in the viscosity of DNA solutions with an increase in the concentration of **6** reveals two linear parts of the plot, i.e., one with a large slope up to $r < 0.1$ and one part with a significantly smaller slope at $r > 0.1$. Thus, it may be proposed that at low ligand-to-DNA ratios, **6** is an intercalator, whereas with increasing r values, a significant contribution of groove binding to the overall association takes place. DNA groove binding does not result in the lengthening of the DNA, and consequently, it does not lead to an increase in the bulk viscosity of the DNA solution, which explains the much lower slope in the plot of the viscosity of the DNA solution versus the ligand-to-DNA ratio at $r > 0.15$.

In contrast to the other DAPS, the partly saturated derivative **7** shows much weaker induced LD signals in the presence of DNA. These signals are negative at low ligand-to-DNA ratios but become positive at higher ligand loading levels. Moreover, the reduced LD spectrum has different values at different ligand-to-DNA ratios. This behavior

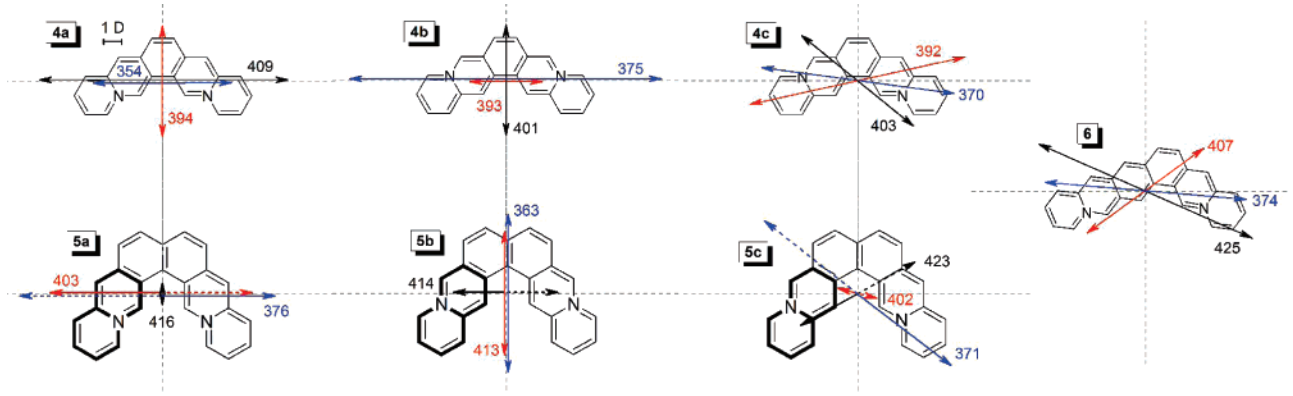

FIGURE 9: Transition dipole moments of the first (black), second (red), and third (blue arrows) lowest-energy electronic transitions of DAPS, as determined by the CI calculations. The dashed parts of the arrows lie behind the paper plane.

indicates that inhomogeneous binding takes place; i.e., at low ligand concentrations, it binds by intercalation with low affinity, whereas at higher concentrations, an additional binding mode, presumably the outside stacking, with a different orientation of the ligand, takes place.

Orientation of the Intercalator within the Binding Pocket. The ICD signals of the ligands that develop upon addition of DNA confirm the interaction of the ligand with the DNA double helix. Moreover, the orientation of an intercalator within the binding pocket may be deduced from the ICD signal, if the intercalator is positioned close to the helix axis. Thus, a positive ICD indicates a perpendicular orientation of the transition dipole moment of the ligand relative to the average dipole moment of the two nucleic bases that constitute the intercalation site, i.e., roughly perpendicular relative to the long axis of the intercalation pocket. A negative ICD indicates a parallel orientation of the transition dipole moment of the ligand relative to the long axis of the binding pocket (*34*, *58*−*60*). This relationship is rather simplifying in many cases and does not take into account symmetry considerations (*61*); however, in most cases, it is sufficient to estimate the structure of the intercalation complex, once the transition dipole moment of the ligand is known. Nevertheless, problems may occur if several transitions overlap or if the orientation of the dipole moments relative to the binding pocket is between 0° and 90°. In the latter case, the intensity of the sign correlates with the square of the cosine of the angle between the transition dipole moment of the ligand and the so-called pseudo-dyad axis of the base pairs (*43*, *58*−*60*).

To discuss the ICD signals that develop upon association of the ligands with DNA, the transition dipole moments of the ligands need to be assessed. Thus, we have performed the configuration−interaction calculations using a semiempirical AM1 Hamiltonian to evaluate the origins of the long-wavelength electronic transitions in DAPS (Figure 9). This method offers an accurate parametrization for polar organic molecules (including heterocyclic compounds) and transition states (*36*, *62*, *63*) and has been widely used for the quantum chemical calculation of cationic organic dyes (*64*−*67*). Moreover, although the relative probabilities of the electronic transitions, calculated by this method, often do not agree with the experimental data, the orientations of the dipole moments and the energies of the electronic transitions show good consistency with the experimental data, especially when a large number of electronic configurations are involved in the calculations (*64*−*67*). In the case of diazoniapentaphenes **4a** and **4b**, which have C_{2v} symmetry, the dipole moments of the three lowest-energy electronic transitions lie in the molecular plane and are parallel to either the long or the short molecular axes. In the case of compound **4c**, the symmetry is broken but the transition dipoles lie in the plane of the chromophore, approximately along the long axis of the chromophore. In the case of methyl-substituted diazoniapentaphenes **4d** and **4e**, the in-plane symmetry is only slightly distorted, and the transition dipole moments are oriented like the ones of the parent diazoniapentaphenes (not shown).

However, the situation is more complicated in the case of diazoniaanthra[1,2-*a*]anthracenes. Derivatives **5a** and **5b** possess C_{2v} symmetry; however, the lateral aromatic rings lie outside the symmetry plane of the cation. Consequently, some of the electronic transitions (in the case of **5c**, all transitions) have non-zero *z* constituents.

To estimate the orientation of ligands **4**−**6** relative to the binding pocket, the above-mentioned relationship between the sign of the ICD of the ligands and the orientation of the corresponding dipole moment was employed. Notably, in most cases, a perfect parallel or perpendicular alignment of the transition dipole moment of the ligand relative to the binding pocket is not possible, because of the steric demands of the ligand. For a qualitative treatment, the following approach was used. (i) The ICD signals of the transitions with the two lowest absorption energies were chosen, with the dipole moments being oriented in significantly different directions. (ii) Considering the size and shape of the ligand, in particular, the steric interactions between ligand and binding site, an orientation of the ligand relative to the long axis of the binding pocket in which both transition dipole moments are as close as possible to the orientation that is expected according to the ICD signal were sought. With this simple model, the structure of the intercalation site was deduced for the representative cases, namely, derivatives **4b**, **4c**, and **5b** (Figure 10). In the case of derivatives **4b** and **4c**, this model leads to almost identical structures; that is, one part of the molecule overlaps with the nucleic bases with an angle of approximately 45° and 60° between the long axis of the naphthalene unit and the long axis of the binding pocket. The remaining azoniaanthracene part of the molecule points outward into the groove with the long axis of the anthracene parallel to the long axis of the binding pocket. Most notably, this binding mode is in agreement with the

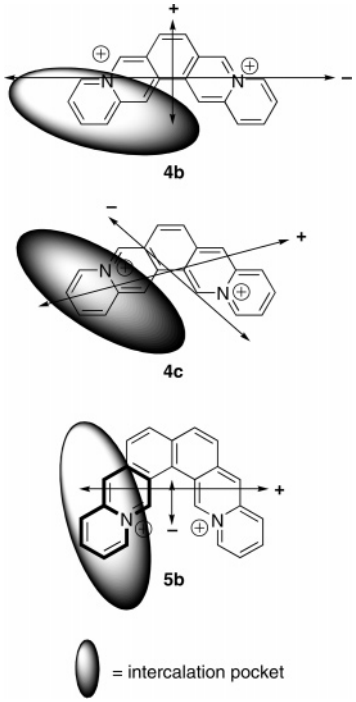

FIGURE 10: Orientation of intercalators **4b**, **4c**, and **5b** relative to the long axis of the intercalation pocket as deduced from the phase of the ICD signals and from the calculated long-wavelength transition dipole moments.

molecular modeling studies of DNA-bound **4e** that show almost the same structure of the intercalation site.

In the case of **5b**, the procedure mentioned above appeared to be difficult, because in the simple two-dimensional model it seems as if it is impossible to fit the intercalator in the binding pocket without the introduction of significant steric interactions between the nonintercalated part of the molecule and the DNA grooves. Nevertheless, a close inspection of the three-dimensional structure of **5b** reveals a helicene-like structure (see details below) that may match the DNA helix. Thus, with one azonianaphthalene part of the ligand intercalated into DNA such as in the case of diazoniapentaphenes **4**, the nonintercalated part, mainly the azoniaanthracene unit, may fit into the helical structure of the grooves. Again, this proposed structure is in good agreement with the theoretical assessment of the binding mode.

Diazoniahexaphene **6** represents an exceptional case in this series. Considering the positive ICD with a maximum at ca. 380 nm that, according to theoretical predictions, corresponds to the third lowest-energy electronic transitions (Figure 9, β band, i.e., $S_0 \rightarrow S_3$ transition), a perpendicular arrangement between the transition moment of the intercalated ligand and the long axis of the binding pocket may be proposed. Nevertheless, especially at $r > 0.2$, the positive ICD signal has an intensity that is significantly higher, i.e., by a factor of 5−10, than the intensities of the ICD signals of derivatives **4** and **5**, although all experiments were performed under identical conditions. As such, a pronounced positive ICD signal usually indicates minor groove binding and usually overlaps the significantly weaker CD signals from intercalated ligands (*33*, *34*); these results support the proposal based on the photometric, LD spectroscopic, and viscosimetric studies (see the discussion above), i.e., that at higher ligand-to-DNA ratios diazoniahexaphene **6** binds to the duplex DNA by groove binding rather than by intercalation.

Overall, the results of the CD spectroscopic analysis of the DNA−ligand complexes give evidence that one common feature of compounds **4** and **5** is the partial intercalation of the diazoniapolycyclic cation with a azonianaphthalene unit into the intercalation site. As there are no additional substituent effects, the shape and size of the remaining part of the ligand determine the overall orientation of the molecule relative to the DNA structure. Apparently, the propensity of the π-system to fit in the groove next to the intercalation site should have a significant influence on the resulting ligand−DNA complex structure and on the strength of the association. This model may also explain why diazoniahexaphene **6** appears not to be a perfect intercalator. With one azonianaphthalene part of **6** intercalated into the helix, the remaining part of the molecule will point outside the binding site to such an extent that it exceeds the outer rim of the DNA. The part of the molecule that is no longer accommodated in the interior of the DNA will experience hydrophobic interactions with the surrounding water molecules, which leads to a decrease in the overall energy of intercalation, so that groove binding becomes a competitive binding mode. Thus, in contrast to intercalators **4** and **5**, the diazoniahexaphene is also to a significant extent a groove binder.

Binding Affinities for the Duplex. We used spectrophotometric titration data and results of the thermal denaturation experiments to evaluate and compare the binding constants for the binding of the ligands to dsDNA. The binding isotherms from the spectrophotometric titrations were fitted to the binding model of McGhee and von Hippel (*30*, *46*), to access the values of the affinity constant, *K*, and the binding site size, *n*, which are given in Table 1. Remarkably, all members of the diazoniapentaphene series (**4a**−**e**) have similar values for the binding constant ($K = 1.2-1.8 \times 10^5$ M^{-1}). This indicates that variation of the position of the nitrogen atoms within the pentaphene framework, as well as introduction of additional methyl groups, does not result in significant changes in the DNA binding affinity. Hexacyclic derivatives **5a**−**c** have significantly higher binding constants ($K \approx 5 \times 10^6$ M^{-1} for compounds **5b** and **5c**). The binding site covers approximately 2 bp for both series **4a**−**e** and **5a**−**c**, which is consistent with the intercalation model.

Stabilization of the DNA Duplex. The results of the thermal denaturation experiments, presented as ligand-induced shifts of the melting temperature of the DNA (ΔT_m), do not directly correlate with the values of association constant of ligands to the DNA, since the ΔT_m values depend also on the binding site size and additional thermodynamic parameters of binding (*54*, *55*). However, since the ligands investigated in this study bear strong structural resemblance and identical net charges (which are independent of the buffer conditions, other than in the case of the charges acquired by the protonation of the amine nitrogens), their thermodynamical parameters of binding may be expected to be very similar. Moreover, the spectrophotometric titration data gave similar values of the binding site size for almost all DAPS. Therefore, we used the ΔT_m values as an appropriate measure to compare the binding affinities of the ligands for DNA. At low ionic strengths (16 mM Na^+), all DAPS, except for derivative **7**, bind to dsDNA and stabilize it against thermal denaturation to a large extent, comparable to or extending the stabilization

observed with other efficient intercalators, such as proflavine (*29*). Consistent with the results of the spectrophotometric titrations, the variation of the position of the quaternary nitrogen atoms in isomers **4a**−**c** does not influence the DNA binding affinity significantly, although compound **4a** exhibits a slightly stronger binding (cf. the ΔT_m values of 19.0, 17.5, and 17.6 °C, respectively, for stabilization of ctDNA at $r = 0.5$). Moreover, all compounds from the diazoniapentaphene series show preferential binding to GC-rich DNA structures. These findings may be rationalized by the assumption that the net charges of the ligands are efficiently delocalized within the aromatic system, and specific interactions, e.g., hydrogen bonding, between the azonia nitrogens and DNA do not take place. The introduction of one or two methyl groups into the diazoniapentaphene framework, such as in derivatives **4d** and **4e**, did not result in pronounced changes in the induced shifts of DNA melting temperatures as compared to the unsubstituted compounds. Therefore, we may conclude that the slight deviations from the planar structure in methyl-substituted diazoniapentaphenes do not have any significant effect on the DNA binding properties.

Diazoniaanthra[1,2-*a*]anthracenes **5a**−**c** and diazoniahexaphene **6** exhibit an even higher degree of stabilization of dsDNA. This observation reflects the fact that, as the net charges of the ligand are identical with pentacyclic compounds **4a**−**e**, the larger aromatic surface area results in an enhanced affinity for dsDNA. At the same time, within the diazoniaanthra[1,2-*a*]anthracenes **5**, a larger variation of affinities and base selectivities is observed than in the diazoniapentaphene series. Thus, compound **5a** shows a stronger stabilization of GC-containing DNA, whereas isomer **5b** stabilizes $[poly(dAdT)]_2$ to a larger extent; in the case of compound **4c**, we inferred no base selectivity. The results of the competition dialysis assay also strongly confirm the preferential binding of **4c** and **5a** to GC-rich dsDNA (*27*).

The melting curves of DNA in the presence of diazoniapolycyles (Figure 5) are biphasic at low ligand-to-DNA ratios ($0 < r \leq 0.2$). This behavior is especially pronounced for the thermal denaturation of DNA in the presence of hexacyclic ligands **5a**−**c**. It has been shown that such a melting curve shape may be due to ligand redistribution from the melted loops to the double-stranded regions of DNA in the course of denaturation and, provided other binding parameters (ligand concentration, binding site size) are similar, becomes especially pronounced for DNA binders with large binding constants (*54*, *55*). Notably, the saturation of the helix lattice takes place only at relatively high *r* values ($r \geq 2$), as reflected by the influence of the ligand-to-DNA ratio on the induced ΔT_m shifts (Figure 5C), while much smaller ratios (e.g., $r = 0.5$) are often termed "saturating" (*29*).

The relatively high affinity of the diazoniahexaphene **6** for $[poly(dAdT)]_2$, as seen from the thermal denaturation data, allows us to expect, in agreement with the CD spectroscopic analysis, an at least partial contribution from the groove binding mode, as the minor groove binders bind preferentially to AT-rich DNA sequences (*68*, *69*). Indeed, the elongated, curved shape of the diazoniahexaphene **6** might facilitate its placement in the minor groove of the DNA; however, the contribution of the hydrogen bonding with the phosphate backbone, which is often important for the groove-binding ligands, cannot take place with the unsubstituted diazoniapolycycles.

Compound **7** represents a dicationic polycycle where a fully aromatic character is distorted by two sp^3-hybridized carbon atoms. Although the net charge of the chromophore and its geometrical size are similar to the ones of diazoniapentaphenes **4b**, the DNA binding parameters of compound **7** are significantly lower than those of fully aromatic diazoniapolycycles (cf. data in Table 2). Notably, in the series of related, cationic protoberberine derivatives, a completely opposite behavior was observed; thus, 5,6-dihydro-8-desmethylcoralyne binds to double-stranded polynucleotides $[poly(dAdT)]_2$ and $[poly(dIdC)]_2$ with much higher affinity than its fully aromatic analogue, 8-desmethylcoralyne, as determined by DNA thermal denaturation studies (*70*).

Binding to the Triplex DNA. Since the triplex DNA is unstable at low ionic strengths in the absence of divalent cations or polyamines, thermal denaturation studies with the poly(dA)-$[poly(dT)]_2$ triplex were performed at a higher salt concentration ($[Na^+] = 200$ mM), which is in accordance with the established procedures (*28*). However, the ΔT_m values, obtained under different ionic strength conditions, cannot be directly used for comparison of the binding affinities of the ligands for DNA, since the melting temperature of DNA depends strongly on the salt concentration even in the absence of ligands (*71*). On the other hand, binding of the ligands to the double-stranded DNA is also salt-dependent due to the counterion release that accompanies the binding (*52*), as illustrated in Figure 6. Therefore, under the conditions of high-ionic strength, which favor the formation of triple-helical DNA, the binding of diazoniapolycycles to dsDNA is significantly weakened.

The diazoniapolycyclic salts efficiently bind to the poly(dA)-$[poly(dT)]_2$ triplex and stabilize it against thermal denaturation, as characterized by the $\Delta T_m^{3\rightarrow2}$ values (Table 3). Most importantly, diazoniapolycycles distinguish between triplex and duplex structures, which can be seen from a comparison of the induced T_m shifts ($\Delta T_m^{3\rightarrow2}$ vs $\Delta T_m^{2\rightarrow1}$). Thus, diazoniapentaphenes **4a**−**e** show very good selectivity at low to near-saturating ligand-to-DNA ratios ($0 < r \leq 0.5$). At the same time, diazoniaanthra[1,2-*a*]anthracenes **5a**−**c** exhibit much higher binding affinity for the poly(dA)-$[poly(dT)]_2$ triplex, which one can see from the thermal denaturation studies and equilibrium dialysis results. Among the hexacyclic derivatives, compound **5a** shows an excellent triplex-versus-duplex selectivity at $r \leq 0.2$; however, at higher ligand concentrations, **5a** and especially **5b** and **5c** bind also to the duplex form. Remarkably, the diazoniahexaphene **6** has very poor triplex-versus-duplex selectivity; in fact, at low ligand-to-DNA ratios ($r \leq 0.2$), it stabilizes triple-helical and double-stranded forms of DNA to a similar extent, while at higher *r* values, binding to the triplex form prevails.

As in the case of the duplex binding, the variation of the position of heteroatoms in the series **4a**−**c** has almost no influence on the triplex binding properties, and the introduction of methyl groups into derivatives **4d** and **4e** results only in minor differences, except for somewhat poorer triplex stabilizing properties in the case of **4e**. It has been shown that the positions of the heteroatoms have a large influence on the triplex DNA binding properties in the series of the pyridoquinoxaline derivatives (*72*) and in the case of

dibenzophenanthrolines (*73*, *74*). However, in the case of the diazoniapolycyclic ions, presented in this study, the heteroatoms are not available for hydrogen bonding with the DNA−phosphate backbone, and the charges contributed by the quaternary nitrogen atoms are efficiently delocalized within the aromatic ring system.

It has been shown that the extension of the aromatic ring system from tetracyclic to pentacyclic hetarenes favors triplex stabilization due to the larger surface area available for the π-stacking interactions (*75*). It may be suggested that, in a similar way, further extension of the π-system from the diazoniapentaphene series to the six-ring diazoniaanthra[1,2-*a*]anthracene structure (**5**) facilitates the triplex binding properties. However, diazoniahexaphene **6** represents an exception from this trend, since, although its aromatic surface area is similar to that of diazoniaanthra[1,2-*a*]anthracenes, it shows much worse selectivity for the triplex DNA compared to the latter compounds. On the other hand, it has been suggested that aminoalkyl-substituted naphthylquinolines, such as **8**, are efficient triplex-DNA binders due to some degree of torsional flexibility in the molecule (*76*). In fact, it was shown by NMR and X-ray diffraction studies of triple-helical DNA structures that the nucleic bases in a base triplet are not coplanar but deviate considerably from the mean plane, inclined by angles of up to 33° ("propeller twist") (*77*−*79*). The diazoniaanthra[1,2-*a*]anthracenes are nonplanar compounds, which may be seen from the X-ray structure analysis of derivative **5c** (*25*). Moreover, the value of an angle between the quinolizinium moieties of the dication (30.7°) matches almost perfectly the propeller twist of the nucleic bases. Therefore, it is suggested that the nonplanarity of diazoniaanthra[1,2-*a*]anthracenes significantly facilitates their interaction with the triple-helical DNA for geometrical reasons. It may be also suggested that binding of these compounds to triplex DNA is associated with a unidirectional *P*/*M* racemization, since the interconversion barrier should be rather low. Thus, this system may be considered as an annelated [4]helicene, the racemization barrier of which was estimated to be about 4 kcal/mol (*80*).

The nonplanarity of the nucleic bases in triple-helical DNA may also be the reason for the reduced triplex-versus-duplex selectivity of diazoniahexaphene **6**, as compared to the diazoniaanthra[1,2-*a*]anthracenes. Thus, its large aromatic surface area favors the interaction with duplex DNA, compared to the five-membered diazoniapentaphenes **4a**−**c**; however, its planar shape does not facilitate the interaction with triplex DNA. Therefore, it may be concluded that a twisted shape of the chromophore is more important for the triplex binding properties than the simple extension of the planar π-system.

It should be noted that the diazoniaanthra[1,2-*a*]anthracene **5a**, which shows the highest triplex-DNA affinity among the diazoniapolycycles investigated in this study, is superior to the triplex-DNA ligands such as the first-generation naphthylquinoline **8** ($\Delta T_m^{3\rightarrow2} \approx 35$ °C and $\Delta T_m^{2\rightarrow1} \approx 5$ °C at $r = 0.2$ under nearly identical conditions) (*76*) (Chart 2). Thus, the $\Delta T_m^{2\rightarrow1}$ values for **5a** are significantly lower, and although the $\Delta T_m^{3\rightarrow2}$ values are slightly larger for the naphthylquinolines, compound **5a** exhibits a significantly higher selectivity for triplex stabilization. This selectivity of diazoniaanthra[1,2-*a*]anthracene **5a** is comparable to that of a recently reported improved series of naphthylquinoline derivatives (*81*). It is also very close to the ligand DB359 from the series of polyaromatic diamidines ($\Delta T_m^{3\rightarrow2} \approx 27$ °C and $\Delta T_m^{2\rightarrow1} \approx 1$ °C at $r = 0.2$ under identical conditions), which has been described as "one of the most triplex-selective compounds discovered" (*82*).

Chart 2: Structures of Known Efficient Triplex Binders

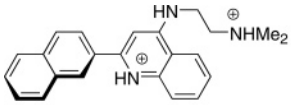

8

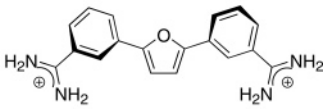

DB359

However, in contrast to the majority of the reported triplex-DNA binders, in the diazoniapolycyclic salts the two full positive charges, which are essential for DNA binding, are located on the aromatic core, and not on protonated nitrogen atoms. Therefore, the overall charge of the intercalator and thus its DNA binding properties are independent of the pH of the environment, excluding strongly alkaline media which may lead to decomposition of azonia salts due to formation of leucobases. Moreover, since protonation is not necessary to realize a positive charge in the DAPS derivatives, the equilibrium between unprotonated and protonated amine functionality, which may interfere with the DNA association, is excluded.

CONCLUSION

In summary, we have shown that diazoniapolycyclic salts are a useful class of compounds that may be used to assess the intrinsic parameters, i.e., the ones that are not influenced by additional substituents, that govern the associative interactions of a ligand with double- and triple-stranded DNA. Diazoniapolycyclic ions represent a structural motif with a high selectivity toward double- and triple-helical DNA structures. The DNA affinity is mainly determined by the shape of the polycyclic system and the two cationic charges, whereas the position of the heteroatoms has little influence on the DNA binding properties. At the same time, the binding mode of these compounds was different, depending on the shape of the polycyclic system.

(i) Angular diazoniapentaphenes **4a**−**e** bind to the duplex form predominantly by the intercalation and preferably to the GC-rich structures. At high ionic strengths, they also bind to the poly(dA)-[poly(dT)]$_2$ triplex with a higher affinity than for the corresponding duplex form.

(ii) The extension of the angular aromatic system to diazoniahexaphene **6** results in a preferential groove binding mode at larger ligand-to-DNA ratios and a preference for AT-rich structures, which form a narrower minor groove. This structural change also greatly weakens the affinity for the triplex DNA, resulting in approximately the same binding to the duplex and triplex. We attribute this behavior to the unfavorable shape of the flat aromatic system, which is larger than the surface of the base pair of the duplex and, on the other hand, does not match the helical twist of the base triplet of the triplex form.

(iii) The helical-shaped diazoniaanthra[1,2-*a*]anthracenes **5a**−**c** bind both to the duplex and to the triplex DNA by intercalation with a high affinity, exceeding that of compounds **4a**−**e**. This behavior is most likely due to the favorable match of the shape of the chromophore, which

allows a partial intercalation into the duplex as well as into the triplex forms.

Moreover, the diazoniapolycyclic salts represent a unique example of the triplex-binding aromatic heterocycles that do not need side-chain substituents and therefore constitute a promising lead structure for the design of drugs whose mode of action involves the stabilization of triplex DNA.

ACKNOWLEDGMENT

We thank Mr. Haixing Li for assistance with the viscosimetric titrations.

SUPPORTING INFORMATION AVAILABLE

Spectrophotometric titrations of DNA to **4b**−**e**, **5a**−**c**, and **7**, along with the corresponding Scatchard plots; melting profiles of poly(dAdT)$_2$, calf thymus DNA, and poly(dA)-[poly(dT)]$_2$ in the presence of **4a**−**e**, **5a**−**c**, **6**, and **7**; and the structure of intercalated **4e** and **5b** derived from molecular modeling. This material is available free of charge via the Internet at http://pubs.acs.org.

REFERENCES

1. Neidle, S., and Waring, M., Eds. (1993) *Molecular Aspects of Anticancer Drug-DNA Interactions*, CRC Press, Boca Raton, FL.
2. D'Incalci, M., and Sessa, C. (1997) DNA minor groove binding ligands: A new class of anticancer agents, *Expert Opin. Invest. Drugs 6*, 875−884.
3. Waring, M. J. (2006) *Sequence-specific DNA binding agents*, RSC Publishing, Cambridge, U.K.
4. Hannon, M. J. (2007) Supramolecular DNA recognition, *Chem. Soc. Rev. 36*, 280−295.
5. Tsai, C. C., Jain, S. C., and Sobell, H. M. (1975) Mutagen-Nucleic Acid Intercalative Binding: Structure of a 9-aminoacridine:5-iodocytidylyl(3′-5′)guanosine Crystalline Complex, *Proc. Natl. Acad. Sci. U.S.A. 72*, 628−632.
6. Davies, D. B., Pahomov, V. I., and Veselkov, A. N. (1997) NMR determination of the conformational and drug binding properties of the DNA heptamer d(GpCpGpApApGpC) in aqueous solution, *Nucleic Acids Res. 25*, 4523−4531.
7. Bailly, C., Arafa, R. K., Tanious, F. A., Laine, W., Tardy, C., Lansiaux, A., Colson, P., Boykin, D. W., and Wilson, W. D. (2005) Molecular Determinants for DNA Minor Groove Recognition: Design of a Bis-Guanidinium Derivative of Ethidium That Is Highly Selective for AT-Rich DNA Sequences, *Biochemistry 44*, 1941−1952.
8. Garbett, N. C., Hammond, N. B., and Graves, D. E. (2004) Influence of the amino substituents in the interaction of ethidium bromide with DNA, *Biophys. J. 87*, 3974−3981.
9. Joseph, J., Kuruvilla, E., Achuthan, A. T., Ramaiah, D., and Schuster, G. B. (2004) Tuning of intercalation and electron-transfer processes between DNA and acridinium derivatives through steric effects, *Bioconjugate Chem. 15*, 1230−1235.
10. Modukuru, N. K., Snow, K. J., Perrin, B. S., Jr., Thota, J., and Kumar, C. V. (2005) Contributions of a Long Side Chain to the Binding Affinity of an Anthracene Derivative to DNA, *J. Phys. Chem. B 109*, 11810−11818.
11. Tan, W. B., Bhambhani, A., Duff, M. R., Rodger, A., and Kumar, C. V. (2006) Spectroscopic identification of binding modes of anthracene probes and DNA sequence recognition, *Photochem. Photobiol. 82*, 20−30.
12. Duff, M. R., Tan, W. B., Bhambhani, A., Perrin, B. S., Jr., Thota, J., Rodger, A., and Kumar, C. V. (2006) Contributions of hydroxyethyl groups to the DNA binding affinities of anthracene probes, *J. Phys. Chem. B 110*, 20693−20701.
13. Becker, H.-C., and Nordén, B. (1999) DNA binding mode and sequence specificity of piperazinylcarbonyloxyethyl derivatives of anthracene and pyrene, *J. Am. Chem. Soc. 121*, 11947−11952.
14. Kumar, C. V., and Asuncion, E. H. (1993) DNA binding studies and site selective fluorescence sensitization of anthryl probe, *J. Am. Chem. Soc. 115*, 8547−8553.
15. Bair, K. W., Tuttle, R. L., Knick, V. C., Cory, M., and McKee, D. D. (1990) [(1-Pyrenylmethyl)amino] alcohols, a new class of antitumor DNA intercalators. Discovery and initial amine side chain structure-activity studies, *J. Med. Chem. 33*, 2385−2393.
16. Ihmels, H., Faulhaber, K., Vedaldi, D., Dall'Acqua, F., and Viola, G. (2005) Intercalation of organic dye molecules into double-stranded DNA Part 2: The annelated quinolizinium ion as a structural motif in DNA intercalators, *Photochem. Photobiol. 81*, 1107−1115.
17. Ihmels, H., Faulhaber, K., Sturm, C., Bringmann, G., Messer, K., Gabellini, N., Vedaldi, D., and Viola, G. (2001) Acridizinium Salts as a Novel Class of DNA-Binding and Site-Selective DNA-Photodamaging Chromophores, *Photochem. Photobiol. 74*, 505−511.
18. Viola, G., Bressanini, M., Gabellini, N., Vedaldi, D., Dall'Acqua, F., and Ihmels, H. (2002) Naphthoquinolizinium derivatives as novel platform for DNA-binding and DNA-photodamaging chromophores, *Photochem. Photobiol. Sci. 1*, 882−889.
19. Ihmels, H., Otto, D., Dall'Acqua, F., Faccio, A., Moro, S., and Viola, G. (2006) Comparative Studies on the DNA-binding Properties of Linear and Angular Dibenzoquinolizinium Ions, *J. Org. Chem. 71*, 8401−8411.
20. Bradsher, C. K., and Parham, J. C. (1964) Diazoniapentaphene Salts, *J. Org. Chem. 29*, 856−858.
21. Krapcho, A. P., and Cadamuro, S. A. (2004) Diazoniapentaphenes. Synthesis from Pyridine-2-carboxaldehyde and Structural Verifications, *J. Heterocycl. Chem. 41*, 291−294.
22. Granzhan, A., Ihmels, H., Mikhlina, K., Deiseroth, H.-J., and Mikus, H. (2005) Synthesis of Substituted Diazoniapentaphene Salts by an Unexpected Rearrangement-Cyclodehydration Sequence, *Eur. J. Org. Chem.*, 4098−4108.
23. Bradsher, C. K., and Sherer, J. P. (1968) Diazonia Hexacyclic Aromatic Systems From bis(Bromomethyl)naphthalenes, *J. Heterocycl. Chem. 5*, 253−257.
24. Fields, D. L., and Regan, T. H. (1973) Overcrowded Molecules. V. 3,10-Dimethyl-1,12-bis(2-pyridyl)benzo[*c*]phenanthrene-2,11-diol, *J. Heterocycl. Chem. 10*, 195−199.
25. Granzhan, A., Bats, J. W., and Ihmels, H. (2006) Synthesis and Spectroscopic Properties of 4a,14a-Diazoniaanthra[1,2-*a*]-anthracene and 13a,16a-Diazoniahexaphene Derived from 2,7-Dimethylnaphthalene, *Synthesis*, 1549−1555.
26. Viola, G., Ihmels, H., Krausser, H., Vedaldi, D., and Dall'Acqua, F. (2004) DNA-binding and DNA-photocleavaging properties of 12a,14a-diazoniapentaphene, *ARKIVOC (Gainesville, FL, U.S.) v*, 219−230.
27. Granzhan, A., and Ihmels, H. (2006) Selective Stabilization of Triple-Helical DNA by Diazoniapolycyclic Intercalators, *ChemBioChem 7*, 1031−1033.
28. Ren, J., and Chaires, J. B. (1999) Sequence and Structural Selectivity of Nucleic Acid Binding Ligands, *Biochemistry 38*, 16067−16075.
29. McConnaughie, A. W., and Jenkins, T. C. (1995) Novel acridine-triazenes as prototype combilexins: Synthesis, DNA binding, and biological activity, *J. Med. Chem. 38*, 3488−3501.
30. Graves, D. E. (2001) Drug-DNA Interaction, in *DNA Topoisomerase Protocols, Methods in Molecular Biology* (Osheroff, N., and Bjornsti, M. A., Eds.) Vol. 95, Part II, pp 161−169, Humana Press, Totowa, NJ.
31. Fukui, K., and Tanaka, K. (1996) The acridine ring selectively intercalated into a DNA helix at various types of abasic sites: Double strand formation and photophysical properties, *Nucleic Acids Res. 24*, 3962−3967.
32. Wada, A., and Kozawa, S. (1964) Instrument for studies of differential flow dichroism of polymer solutions, *J. Polym. Sci., Part A: Polym. Chem. 2*, 853−864.
33. Nordén, B., Kubista, M., and Kurucsev, T. (1992) Linear dichroism spectroscopy of nucleic acids, *Q. Rev. Biophys. 25*, 51−170.
34. Nordén, B., and Kurucsev, T. (1994) Analysing DNA complexes by circular and linear dichroism, *J. Mol. Recognit. 7*, 141−156.
35. Frisch, M. T. G. W., Schlegel, H., Scuseria, G., Robb, M., Cheeseman, J., Zakrzewski, V., Montgomery, J., Stratmann, R. E., Burant, J. C., Dapprich, S., Millam, J., Daniels, A., Kudin, K., Strain, M., Farkas, O., Tomasi, J., Barone, V., Cossi, M., Cammi, R., Mennucci, B., Pomelli, C., Adamo, C., Clifford, S., Ochterski, J., Petersson, G. A., Ayala, P. Y., Cui, Q., Morokuma, K., Malick, D. K., Rabuck, A. D., Raghavachari, K., Foresman, J. B., Cioslowski, J., Ortiz, J. V., Stefanov, B. B., Liu, G., Liashenko, A., Piskorz, P., Komaromi, I., Gomperts, R., Martin, R. L., Fox, D. J., Keith, T., Al-Laham, M. A., Peng, C. J.,

Nanayakkara, A., Gonzalez, C., Challacombe, M., Gill, P. M. W., Johnson, B. G., Chen, W., Wong, M. W., Andres, J. L., Head-Gordon, M., Replogle, E. S., and Pople, J. A. (1998) *Gaussian 98*, revision A.6, Gaussian, Inc., Pittsburgh, PA.

36. Dewar, M. J. S., Zoebisch, E. G., Healy, E. F., and Stewart, J. J. P. (1985) Development and use of quantum mechanical molecular models. 76. AM1: A new general purpose quantum mechanical molecular model, *J. Am. Chem. Soc. 107*, 3902−3909.
37. Carter, E. S. II, and Tung, C. S. (1996) *NAMOT2* - a redesigned nucleic acid modeling tool: construction of non-canonical DNA structures. *Comput. Appl. Biosci. 12*, 25−30.
38. *MOE (The Molecular Operating Environment)*, version 2005.06, Chemical Computing Group Inc., Montreal, QC, 2005.
39. Cornell, W. D., Cieplak, P., Bayly, C. I., Gould, I. R., Merz, K. M., Ferguson, D. M., Spellmeyer, D. C., Fox, T., Caldwell, J. W., and Kollman, P. A. (1995) A Second Generation Force Field for the Simulation of Proteins, Nucleic Acids, and Organic Molecules, *J. Am. Chem. Soc. 117*, 5179−5197.
40. Qiu, D., Shenkin, P. S., Hollinger, F. P., and Still, W. C. (1997) The GB/SA continuum model for solvation. A fast analytical method for the calculation of approximate Born radii, *J. Phys. Chem. A 101*, 3005−3014.
41. Baxter, C. A., Murray, C. W, Clark, D. E., Westhead, D. R., and Eldridge, M. D. (1998) Flexible docking using TABU search and an empirical estimate of binding affinity, *Proteins: Struct., Funct., Genet. 33*, 367−382.
42. Halgren, T. A. (1999) MMFF VII. Characterization of MMFF94, MMFF94s, and other widely available force fields for conformational energies and for intermolecular-interaction energies and geometries, *J. Comput. Chem. 20*, 730−748.
43. Kollman, P. A., Massova, I., Reyes, C., Kuhn, B., Huo, S. H., Chong, L., Lee, M., Lee, T., Duan, Y., Wang, W., Donini, O., Cieplak, P., Srinivasan, J., Case, D. A., and Cheatham, T. E. (2000) Calculating structures and free energies of complex molecules: Combining molecular mechanics and continuum models, *Acc. Chem. Res. 33*, 889−897.
44. Onufriev, A., Bashford, D., and Case, D. A. (2000) Modification of the generalized Born model suitable for macromolecules, *J. Phys. Chem. B 104*, 3712−3720.
45. *HyperChem 7.51*, Hypercube, Inc., Gainesville, FL, 2002.
46. McGhee, J. D., and von Hippel, P. H. (1974) Theoretical aspects of DNA-Protein interactions: Cooperative and non-cooperative binding of large ligands to a one-dimensional homogeneous lattice, *J. Mol. Biol. 86*, 469−489.
47. Cohen, G., and Eisenberg, H. (1969) Viscosity and Sedimentation Study of Sonicated DNA-Proflavine Complexes, *Biopolymers 8*, 45−55.
48. Suh, D., and Chaires, J. B. (1995) Criteria for the mode of binding of DNA binding agents, *Bioorg. Med. Chem. 3*, 723−728.
49. Lerman, L. S. (1961) Structural considerations in the interaction of DNA and the acridines, *J. Mol. Biol. 3*, 18−30.
50. Reddy, B. S., Seshadri, T. P., Sakore, T. D., and Sobell, H. M. (1979) Visualization of drug−nucleic acid interactions at atomic resolution. V. Structure of two aminoacridine−dinucleoside monophosphate crystalline complexes, proflavine-5-iodocytidylyl (3′-5′) guanosine and acridine orange-5-iodocytidylyl (3′-5′) guanosine, *J. Mol. Biol. 135*, 787−812.
51. Aslanoglu, M. (2006) Electrochemical and Spectroscopic Studies of the Interaction of Proflavine with DNA, *Anal. Sci. 22*, 439−443.
52. Owczarzy, R., You, Y., Moreira, B. G., Manthey, J., Huang, L., Behlke, M. A., and Walder, J. A. (2004) Effects of Sodium Ions on DNA Duplex Oligomers: Improved Predictions of Melting Temperatures, *Biochemistry 43*, 3537−3554.
53. Record, M. T., Lohman, T. M., and de Haseth, P. (1976) Ion effects on ligand−nucleic acid interactions, *J. Mol. Biol. 107*, 145−158.
54. McGhee, J. D. (1976) Theoretical calculations of the helix-coil transition of DNA in the presence of large, cooperatively binding ligands, *Biopolymers 15*, 1345−1375.
55. Spink, C. H., and Wellman, S. E. (2001) Thermal denaturation as tool to study DNA-ligand interactions, *Methods Enzymol. 340*, 193−211.
56. Schildkraut, C., and Lifson, S. (1965) Dependence of the melting temperature of DNA on salt concentration, *Biopolymers 3*, 195−208.
57. Scaria, P. V., and Shafer, R. H. (1991) Binding of ethidium bromide to a DNA triple helix. Evidence for intercalation, *J. Biol. Chem. 266*, 5417−5423.
58. Norden, B., and Tjerneld, F. (1982) Structure of methylene blue-DNA complexes studied by linear and circular dichroism spectroscopy, *Biopolymers 21*, 1713−1734.
59. Lyng, R., Rodger, A., and Norden, B. (1991) The CD of ligand-DNA systems. I. Poly(dG-dC) B-DNA, *Biopolymers 31*, 1709−1820.
60. Schipper, P. E., Norden, B., and Tjerneld, F. (1980) Determination of binding geometry of DNA-adduct systems through induced circular dichroism, *Chem. Phys. Lett. 70*, 17−21.
61. Schipper, E. P., and Rodger, A. (1983) Symmetry rules for the determination of the intercalation geometry of host/systems using circular dichroism: A symmetry-adapted coupled-oscillator model, *J. Am. Chem. Soc. 105*, 4541−4150.
62. Dewar, M. J. S., and Dieter, K. M. (1986) Evaluation of AM1 calculated proton affinities and deprotonation enthalpies, *J. Am. Chem. Soc. 108*, 8075−8086.
63. Stewart, J. J. P. (1990) A semiempirical molecular orbital program, *J. Comput.-Aided Mol. Des. 4*, 1−103.
64. Clark, T. (1993) Semiempirical molecular orbital theory: Facts, myths and legends, in *Recent Experimental and Computational Advances in Molecular Spectroscopy* (Fausto, R., Ed.) Vol. 406, pp 369−380, Kluwer, Dordrecht, The Netherlands.
65. McCarthy, P. K., and Blanchard, G. J. (1993) AM1 study of the electronic structure of coumarins, *J. Phys. Chem. 97*, 12205−12209.
66. Rodríguez, J., Scherlis, D., Estrin, D., Aramendía, P. F., and Negri, R. M. (1997) AM1 Study of the Ground and Excited State Potential Energy Surfaces of Symmetric Carbocyanines, *J. Phys. Chem. A 101*, 6998−7006.
67. Peszke, J., and Śliwa, W. (2002) AM1 CI and ZINDO/S study of quaternary salts of diazaphenanthrenes with haloalkanes, *Spectrochim. Acta, Part A 58*, 2127−2133.
68. Mallena, S., Lee, M. P. H., Bailly, C., Neidle, S., Kumar, A., Boykin, D. W., and Wilson, W. D. (2004) Thiophene-Based Diamidine Forms a "Super" AT Binding Minor Groove Agent, *J. Am. Chem. Soc. 126*, 13659−13669.
69. Armitage, B. A. (2005) Cyanine Dye−DNA Interactions: Intercalation, Groove Binding, and Aggregation, *Top. Curr. Chem. 253*, 55−76.
70. Pilch, D. S., Yu, C., Makhey, D., LaVoie, E. J., Srinivasan, A. R., Olson, W. K., Sauers, R. R., Breslauer, K. J., Geacintov, N. E., and Liu, L. F. (1997) Minor Groove-Directed and Intercalative Ligand-DNA Interactions in the Poisoning of Human DNA Topoisomerase I by Protoberberine Analogs, *Biochemistry 36*, 12542−12553.
71. Owczarzy, R., You, Y., Moreira, B. G., Manthey, J., Huang, L., Behlke, M. A., and Walder, J. A. (2004) Effects of Sodium Ions on DNA Duplex Oligomers: Improved Predictions of Melting Temperatures, *Biochemistry 43*, 3537−3554.
72. Escudé, C., Nguyen, C.-H., Kukureti, S., Janin, Y., Sun, J.-S., Bisagni, E., Garestier, T., and Hélène, C. (1998) Rational design of a triple helix-specific intercalating ligand, *Proc. Natl. Acad. Sci. U.S.A. 95*, 3591−3596.
73. Teulade-Fichou, M.-P., Perrin, D., Boutorine, A., Polverari, D., Vigneron, J.-P., Lehn, J.-M., Sun, J.-S., Garestier, T., and Hélène, C. (2001) Direct Photocleavage of HIV-DNA by Quinacridine Derivatives Triggered by Triplex Formation, *J. Am. Chem. Soc. 123*, 9283−9292.
74. Baudoin, O., Marchand, C., Teulade-Fichou, M.-P., Vigneron, J.-P., Sun, J.-S., Garestier, T., Hélène, C., and Lehn, J.-M. (1998) Stabilization of DNA Triple Helices by Crescent-Shaped Dibenzophenanthrolines, *Chem.—Eur. J. 4*, 1504−1508.
75. Nguyen, C. H., Marchand, C., Delage, S., Sun, J.-S., Garestier, T., Hélène, C., and Bisagni, E. (1998) Synthesis of 13*H*-Benzo-[6,7]- and 13*H*-Benzo[4,5]indolo[3,2-*c*]-quinolines: A New Series of Potent Specific Ligands for Triplex DNA, *J. Am. Chem. Soc. 120*, 2501−2507.
76. Wilson, W. D., Tanious, F. A., Mizan, S., Yao, S., Kiselyov, A. S., Zon, G., and Strekowski, L. (1993) DNA triple-helix specific intercalators as antigene enhancers: Unfused aromatic cations, *Biochemistry 32*, 10614−10621.
77. Frank-Kamenetskii, M. D., and Mirkin, S. M. (1995) Triplex DNA structures, *Annu. Rev. Biochem. 64*, 65−95.
78. Vlieghe, D., Van Meervelt, L., Dautant, A., Gallois, B., Precigoux, G., and Kennard, O. (1996) Parallel and antiparallel $(G{\cdot}GC)_2$ triple helix fragments in a crystal structure, *Science 273*, 1702−1705.

79. Thuong, N. T., and Helene, C. (1993) Sequence-specific recognition and modification of double-helical DNA by oligonucleotides, *Angew. Chem., Int. Ed. 32*, 666−690.
80. Grimme, S., and Peyerimhoff, S. D. (1996) Theoretical study of the structures and racemization barriers of [n]helicenes (n=3−6,8), *Chem. Phys. 204*, 411−417.
81. Strekowski, L., Hojjat, M., Wolinska, E., Parker, A. N., Paliakov, E., Gorecki, T., Tanious, F. A., and Wilson, W. D. (2005) New triple-helix DNA stabilizing agents, *Bioorg. Med. Chem. Lett. 15*, 1097−1100.
82. Chaires, J. B., Ren, J., Hamelberg, D., Kumar, A., Pandya, V., Boykin, D. W., and Wilson, W. D. (2004) Structural selectivity of aromatic diamidines, *J. Med. Chem. 47*, 5729−5742.

BI701518V